MOLECULAR ONCOLOGY 9 (2015) 1580–1598

available at www.sciencedirect.com

ScienceDirect

www.elsevier.com/locate/molonc

TIPIN depletion leads to apoptosis in breast cancer cells

Céline Baldeyron[a,b], Amélie Brisson[a,b], Bruno Tesson[a,b,c,d], Fariba Némati[a,e], Stéphane Koundrioukoff[a,f,g], Elie Saliba[a,b], Leanne De Koning[a,h], Elise Martel[i], Mengliang Ye[a,b], Guillem Rigaill[j], Didier Meseure[i], André Nicolas[i], David Gentien[a,k], Didier Decaudin[a,e], Michelle Debatisse[a,f,g], Stéphane Depil[l], Francisco Cruzalegui[l,1], Alain Pierré[l], Sergio Roman-Roman[a,b], Gordon C. Tucker[l], Thierry Dubois[a,b,*]

[a]Institut Curie, Centre de Recherche, Paris, F-75248, France
[b]Breast Cancer Biology Group, Department of Translational Research, Paris, F-75248, France
[c]INSERM, U900, Bioinformatics, Biostatistics, Epidemiology and Computational Systems Biology of Cancer, Paris, F-75248, France
[d]Mines ParisTech, Fontainebleau, F-77300, France
[e]Laboratory of Preclinical Investigation, Department of Translational Research, Paris, F-75248, France
[f]CNRS, UMR 3244, Paris, F-75248, France
[g]Université Pierre and Marie Curie Paris VI, Paris, F-75005, France
[h]RPPA Platform, Department of Translational Research, Paris, F-75248, France
[i]Institut Curie, Investigative Pathology Platform, Paris, F-75248, France
[j]Unité de Recherche en Génomique Végétale, INRA-CNRS-Université d'Evry Val d'Essonne, Evry, F-91057, France
[k]Platform of Molecular Biology Facilities, Department of Translational Research, Paris, F-75248, France
[l]Institut de Recherches SERVIER, Pôle Innovation Thérapeutique Oncologie, Croissy-sur-Seine, F-78290, France

ARTICLE INFO

Article history:
Received 23 October 2014
Received in revised form
10 March 2015
Accepted 23 April 2015
Available online 9 May 2015

Keywords:
Apoptosis
Basal-like
Replicative stress

ABSTRACT

Triple-negative breast cancer (TNBC) is the breast cancer subgroup with the most aggressive clinical behavior. Alternatives to conventional chemotherapy are required to improve the survival of TNBC patients. Gene-expression analyses for different breast cancer subtypes revealed significant overexpression of the Timeless-interacting protein (TIPIN), which is involved in the stability of DNA replication forks, in the highly proliferative associated TNBC samples. Immunohistochemistry analysis showed higher expression of TIPIN in the most proliferative and aggressive breast cancer subtypes including TNBC, and no TIPIN expression in healthy breast tissues. The depletion of TIPIN by RNA interference impairs the proliferation of both human breast cancer and non-tumorigenic cell lines. However, this effect may be specifically associated with apoptosis in breast cancer cells. TIPIN silencing results in higher levels of single-stranded DNA (ssDNA), indicative of

Abbreviations: 2D, 2-dimensional; 3D, 3-dimensional; BC, breast cancer; BrdU, 5-bromo-2′-deoxyuridine; CldU, 5-chloro-2′-deoxyuridine; CN, copy number; DSBs, DNA double-strand breaks; dsDNA, double-stranded DNA; ER, estrogen receptor; HER2, human epidermal growth factor receptor 2; IB, immunoblotting; IdU, 5-iodo-2′-deoxyuridine; IF, immunofluorescence; IOD, inter-origin distance; ITD, inter-termination distance; LA, luminal A; LB, luminal B; PCNA, proliferating cell nuclear antigen; PR, progesterone receptor; RFC, replication fork protection complex; RNAi, RNA interference; RPA, replication protein A; RPPA, reverse phase protein array; ssDNA, single-stranded DNA; TIM, Timeless; TIPIN, TIM-interacting protein; TNBC, triple-negative breast cancer.

* *Corresponding author.* Institut Curie, Centre de Recherche, Département de Recherche Translationnelle, Equipe "Biologie du Cancer du Sein", 26 rue d'Ulm, 75248, Paris Cedex 05, France. Tel.: +33 (0)1 56 24 62 50.
E-mail address: thierry.dubois@curie.fr (T. Dubois).
[1] Present address: Oncology iMED, Translational Science, AstraZeneca, Cheshire, United Kingdom.

http://dx.doi.org/10.1016/j.molonc.2015.04.010

Therapeutic target
TIPIN
Triple-negative breast cancer

replicative stress (RS), in TNBC compared to non-tumorigenic cells. Upon TIPIN depletion, the speed of DNA replication fork was significantly decreased in all BC cells. However, TIPIN-depleted TNBC cells are unable to fire additional replication origins in response to RS and therefore undergo apoptosis. TIPIN knockdown in TNBC cells decreases tumorigenicity *in vitro* and delays tumor growth *in vivo*. Our findings suggest that TIPIN is important for the maintenance of DNA replication and represents a potential treatment target for the worst prognosis associated breast cancers, such as TNBC.

1. Introduction

Breast cancer (BC) is one of the most common tumors in women. It is a complex, heterogeneous disease comprising several subgroups of pathologies with different patient outcomes (Cancer Genome Atlas, 2012; Curtis et al., 2012; Sorlie et al., 2001). Triple-negative breast cancer (TNBC), characterized by an absence of estrogen receptor (ER) and progesterone receptor (PR) expression and a lack of human epidermal growth factor receptor 2 (HER2) overexpression/amplification, has a poor prognosis. TNBC itself constitutes a heterogeneous group of BC (Lehmann et al., 2011; Metzger-Filho et al., 2012; Shah et al., 2012), which is highly proliferative and genetically instable. The treatment of patients with TNBC remains a major clinical challenge. Indeed, unlike other BC subtypes, such as luminal A (LA), luminal B (LB) (both expressing ER and PR) and HER2-overexpressing (Her2) tumors, TNBC cannot be treated with targeted therapies, such as tamoxifen or anti-HER2 antibodies. TNBC patients are therefore treated exclusively with conventional cytotoxic therapies, but about half of them present relapse and metastasis within the first three to five years after treatment (Liedtke et al., 2008). Several molecules are currently being tested in clinical trials, but the identification of new targets for the treatment of TNBC remains crucial (Turner and Reis-Filho, 2013).

For accurate DNA replication, cells need fork protection mechanisms to remove structural obstacles blocking DNA replication (Branzei and Foiani, 2010), so as to ensure the progression of DNA synthesis. Cells must also be able to stabilize stalled replication forks, to prevent dissociation of the DNA replication machinery and to ensure the rapid resumption of replication (Branzei and Foiani, 2010). DNA replication stress (RS), which is defined as an inefficient DNA replication that causes DNA replication forks to progress slowly or stall, is observed in various types of cancer (Bartek et al., 2012; Lecona and Fernandez-Capetillo, 2014; Macheret and Halazonetis, 2015). The factors involved in DNA replication fork stability are potential targets for cancer therapy (Bartek et al., 2012), particularly for highly proliferative and genetically unstable cancers. Timeless (TIM) and its partner TIM-interacting protein (TIPIN) are part of the replication fork protection complex (RFC) (Gotter et al., 2007; Leman et al., 2010) and participate in normal DNA replication to maintain genomic stability (Urtishak et al., 2009). The TIM-TIPIN complex interacts with components of the replication machinery, such as proliferating cell nuclear antigen (PCNA) (Kemp et al., 2010) and replication protein A (RPA) (Ali et al., 2010). TIM-TIPIN plays an important role in coordinating replicative helicases and polymerases to prevent the accumulation of single-stranded DNA (ssDNA) (Gotter et al., 2007).

We found that mRNA levels for TIPIN were significantly higher in TNBC samples than in specimens from other BC subgroups and healthy tissues. In contrast, immunohistochemistry (IHC) analysis revealed that TIPIN was equally expressed at a protein level in the most aggressive and proliferative breast cancer subtypes (TNBC, Her2, LB), with higher expression levels compared to the less proliferative and good prognosis associated LA tumors. In addition, the IHC experiment showed that TIPIN was not expressed in healthy breast tissues. We investigated the potentially deleterious effects of TIPIN depletion on the viability of BC cell lines. We found that the depletion of TIPIN by RNA interference (RNAi) severely compromised the proliferation of human BC and non-tumorigenic cell lines. However, this effect on cell proliferation was mainly associated with apoptosis in TIPIN-depleted BC cells. TIPIN silencing leads to an increase in H2AX phosphorylation during S phase and slower DNA replication kinetics, both of which occur in a more pronounced manner in TNBC cells than in non-cancerous cells. Finally, we found that TIPIN depletion decreased the tumorigenicity of TNBC cells, as shown by the lower number of anchorage-independent colonies and the slower tumor growth in xenograft models. Together, these results suggest that TIPIN represents a potential target for the treatment of poor prognosis associated BC, such as TNBC.

2. Materials and methods

2.1. Human samples and microarray data

Our cohort was composed of 35 LA, 40 LB, 33 Her2, 46 TNBC, and 17 normal breast tissues (Maire et al., 2013a, 2013b). Experiments were performed in accordance with Bioethics Law No. 2004-800 and the Ethics Charter of the French National Cancer Institute (INCa), with the approval of the ethics committee of our institution. Informed consent was not required. The women were informed of the use of their tissues for research and did not oppose this research. DNA (Affymetrix SNP6.0), RNA (Affymetrix U133 Plus 2.0) and RPPA microarrays were performed as described (Maire et al., 2013a; Marty et al., 2008).

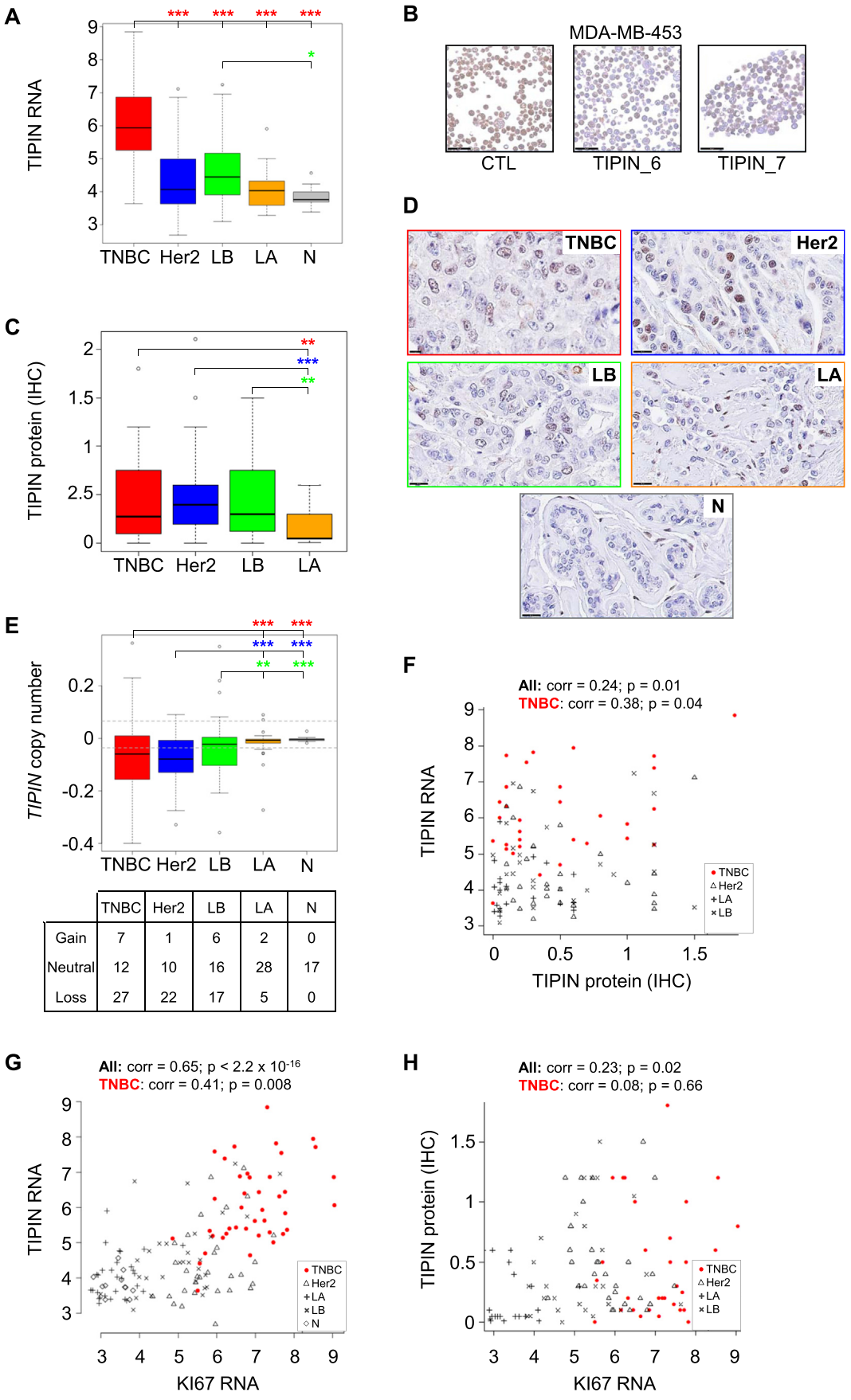

	TNBC	Her2	LB	LA	N
Gain	7	1	6	2	0
Neutral	12	10	16	28	17
Loss	27	22	17	5	0

Figure 1 – TIPIN expression in breast cancer samples. *TIPIN* expression (A–D) and copy number (E) were measured in TNBC (red), Her2 (blue), LB (green), LA (orange) and healthy (N) (gray) breast tissues. (A) TIPIN mRNA levels were determined by microarray analysis. (B) Validation of

2.2. Immunohistochemistry

TIPIN immunohistochemistry (IHC) staining was carried out on tissue microarrays (TMA) containing alcohol, formalin and acetic acid (AFA)-fixed paraffin-embedded tissue as described (Maire et al., 2013a, 2013b). Paraffin sections (3 mm thick) of TMA were deparaffinized before heat-induced epitope retrieval: heating for 20 min at 90°C in DakoCytomation FLEX Target Retrieval Solution, low pH (pH 6) (DAKO). Then, endogenous activity was blocked with Dako REAL™ Peroxidase-Blocking solution (DAKO) followed by an incubation with rabbit polyclonal antibody for TIPIN (GTX129308; GeneTEX) at a dilution of 1/600. Staining was detected with Dako Envision + Dual Link System-HRP (DAKO) with diaminobenzidine as chromogen. Slides were counterstained with hematoxylin before mounting. We carried out all reactions using an automated stainer (Microm Labvision). Negative controls consisted in the omission of the primary antibody. We validated the TIPIN antibody and optimized IHC conditions using AFA-fixed cell pellets from MDA-MB-453 treated with TIPIN siRNA (2 separate siRNA) or control siRNA. Slide sections were acquired with a Philips ultra-fast scanner and then images at × 40 or × 80 magnification were generated. For TIPIN quantification (score = 0–3), we combined the percentage of stained cells (0–100%) with an intensity score (score 0: negative staining; score: 1, 2, 3: weak, intermediate, high nuclear staining, respectively).

2.3. Cell culture, RNA interference and cellular assays

The cell lines were purchased from the American Type Culture Collection cell lines (ATCC, LGC Promochem, Molsheim, France), authenticated in 2013 by short tandem repeat profiling (data not shown) and cultured as described (Maire et al., 2013a). Cells were transfected with 20 nM siRNA (Qiagen, Courtaboeuf, France) as described (Maire et al., 2013a, 2013b; Marty et al., 2008): control (CTL; AllStars negative control, 1027281), TIPIN_6 (5′-AAGCTTGGCGTTACTATGTAT-3′, SI02777915), TIPIN_7 (5′-CTGAGTTAAGTAGAAGCCTAA-3′, SI02777922). We determined cell proliferation by MTT (Roche, Meylan, France) or WST1 (Millipore, Saint Quentin en Yvelines, France) assays and Caspase 3/7 activity by IB as reported (Maire et al., 2013a, 2013b). We performed cell cycle analysis and annexin V staining as described (Maire et al., 2013a). For soft-agar colony formation, 0.35% agar containing siRNA-transfected MDA-MB-468 and HCC70 cells was overlaid onto precast 0.5% bottom agar and incubated 4 weeks as described (Maire et al., 2013a). Three-dimensional (3D) cell culture was performed with Matrigel (BD Biosciences) as described (Maire et al., 2013b). We processed cells for immunostaining as reported (Baldeyron et al., 2011).

2.4. Antibodies

The primary antibodies used in the RPPA, IB, IHC and IF experiments are listed below:

Rabbit anti-β-actin (IB, 1:5000; A2668, Sigma–Aldrich) (Marty et al., 2008), used as loading control; rat anti-BrdU (IF, 1:200; OBT0030, Abcys, Eurobio) (Quivy et al., 2004); rabbit anti-cleaved caspase 3 (IB, 1:1000; E83-77; 1476, Epitomics Inc.) (Maire et al., 2013b); rabbit anti-GRB2 (IB, 1:5000; Y237; 1517, Epitomics Inc.) (Chang et al., 2013); mouse anti-γH2AX (IB, 1:4000; IF, 1:2000; 05-636, Upstate, Millipore) (Lukas et al., 2003); rabbit anti-γH2AX (IF, 1:2000; EP854(2)Y; 2212, Epitomics Inc., Abcam) (Lou et al., 2012); mouse anti-cleaved PARP (IB, 1:1000; 9546, Cell Signaling Technology) (Marty et al., 2008); mouse anti-PCNA (IF, 1:1 000, needs post-fixation in ice-cold methanol for 20 min at −20 °C; PC10; M0879, DAKO) (Green and Almouzni, 2003); rat anti-RPA2 (IF, 1:1000; 2208, Cell Signaling Technology) (Cerqueira et al., 2009); rabbit anti-TIPIN (IB, 1:500; A301-473, Bethyl Laboratories Inc.) (Smith-Roe et al., 2013); rabbit anti-TIPIN (IHC, 1:600); rabbit anti-TIM (IB, 1:5000; IF, 1:1000; 3709; Epitomics Inc., Abcam).

The secondary antibodies used were: For IB or RPPA, HRP-conjugated affinity-purified goat anti-mouse or anti-rabbit (1:20 000; Jackson ImmunoResearch Laboratories, Inc., Interchim). For IF, donkey anti-mouse, anti-rabbit or anti-rat, coupled to Alexa Fluor® 488 or 543 (1:1000; Molecular Probes, Life Technologies).

2.5. Detection of single-stranded DNA (ssDNA)

Cells were cultured in a medium containing 10 μM 5-bromo-2′-deoxyuridine (BrdU; B9285, Sigma–Aldrich, Saint Quentin Fallavier, France) as previously described (Raderschall et al., 1999). After Triton-extraction and fixation, we detected the ssDNA patches by BrdU immunostaining without DNA denaturation. We revealed the total BrdU incorporation into double-stranded DNA (dsDNA) by denaturation with 4 M HCl for 10 min.

TIPIN antibodies for immununohistochemistry (IHC) analysis. Validation of the TIPIN antibody using AFA-fixed cell pellets from MDA-MB-453 treated with control siRNA (left panel) or with 2 distinct TIPIN siRNA (middle and right panels). TIPIN displayed a nuclear localization. Scale bar, 50 μm. (C) Quantitative analysis of the expression of TIPIN at a protein level (IHC) in human breast cancer tissues (quantification score = 0–3) (D) Cellular detection of TIPIN within breast cancer biopsies by IHC. Illustration of TIPIN protein expression (IHC) in the different breast cancer subtypes (with high TIPIN expression) and in healthy breast tissue. TIPIN displayed a nuclear localization. Scale bar, 20 μm. (E) *TIPIN* copy numbers (CN) were determined by microarray analysis. The dashed lines indicate the thresholds retained for the definition of CN gain and loss. The numbers of tumors displaying a loss, a normal number or a gain of *TIPIN* copies are presented in the table. (F) Correlation between TIPIN RNA and protein (IHC) levels. (G) Correlation between TIPIN RNA and Ki67 RNA levels. (H) Correlation between TIPIN protein (IHC) and Ki67 RNA levels. mRNA and DNA copy number relative quantifications were logarithmic (log2) transformed and illustrated by boxplots (A,E). For the statistical analyses, Student's *t* test was used to compared RNA and protein expression levels between 2 groups (TNBC, Her2, LB, LA, N) (A,C), and Fisher's tests for DNA CN comparisons (E). The association between two variables was assessed by Spearman's rank correlation analysis (F–H). The p values are indicated (*$p < 0.05$; **$p < 0.01$; ***$p < 0.001$).

2.6. DNA combing

After pulse labelling of cells with 20 μM 5-iodo-2′-deoxyuridine (IdU) and with 100 μM 5-chloro-2′-deoxyuridine (CldU) for 30 min, we performed DNA combing as described (Anglana et al., 2003; Techer et al., 2013).

2.7. Mice and tumor growth measurement

We injected 4×10^6 viable siRNA-transfected cells subcutaneously into female Swiss nude mouse (Charles River, L'Arbresle, France). Tumor growth was evaluated with a caliper twice a week as described (Maire et al., 2013b). The care and use of these mice complied with internationally established principles of replacement, reduction and refinement, and were in accordance with UKCCCR guidelines (Workman et al., 2010).

2.8. Statistical analysis

Spearman correlation was used to estimate an association between two variables. Data shown in cellular assays and *in vivo* experiments result from at least two independent experiments and the p values were calculated using the Student's *t* test. For DNA combing data, the p values were calculated using the Mann–Whitney test.

3. Results

3.1. High TIPIN protein expression in the poor prognosis associated breast tumors

There is growing interest in the targeting of DNA replication in anti-tumor strategies (Ma et al., 2012; Toledo et al., 2011). We tried to identify genes encoding proteins involved in replication fork stability and displaying overexpression in TNBC, with the aim of discovering new treatment targets for this BC subgroup. We carried out gene-expression profiling on a cohort of normal human breast tissues and BC biopsy specimens, in which all BC subtypes, TNBC, Her2, luminal B (LB) and luminal A (LA), are represented with a similar frequency (Maire et al., 2013a, 2013b). Among several proteins involved in the intra-S checkpoint (Supplementary Figure 1), we found that mRNA levels for TIPIN were significantly higher in TNBC biopsies than in samples from patients with other types of BC or in healthy tissues (Figure 1A). Higher levels of TIPIN RNA were also observed in LB tumors compared to healthy breast tissues (Figure 1A). TIM, the partner of TIPIN, was expressed at similar RNA levels in TNBC, Her2 and LB tumors, with higher expression compared to LA tumors (Supplementary Figure 2A). RPPA analysis revealed that TIM protein was also higher expressed in TNBC, Her2 and LB tumors compared to LA tumors, but with the highest expression levels in TNBC (Supplementary Figure 2B). We were unable to evaluate TIPIN protein level, in the same way, because no antibodies were suitable for RPPA (data not shown). In contrast, using a TIPIN antibody that we first validated for IHC staining (Figure 1B), IHC analysis revealed that TIPIN protein was expressed at similar levels in the most aggressive tumors (TNBC, Her2, LB), with higher levels compared to LA tumors (Figure 1C). The level of TIPIN expression was very heterogeneous between samples within a same tumor subgroup (Figure 1C). TIPIN staining was observed in the nucleus of tumor cells (Figure 1B–D) as reported (Schepeler et al., 2013), and not in healthy breast epithelial cells (Figure 1D). We occasionally observed that TIPIN was expressed in scattered cells in the stromal environment (Figure 1D, image N), as previously reported (Schepeler et al., 2013). These cells corresponded to myoepithelial cells (Figure 1 D). The copy numbers (CN) of *TIPIN* and TIM were, respectively, lower in TNBC, Her2 and LB tumors, and in TNBC tumors, compared to normal breast tissues (Figure 1E), suggesting that the high levels of TIPIN protein in BC do not result from genomic gains. The TIPIN RNA and protein levels correlated weakly in the whole cohort of tumors and within the TNBC subtype (Figure 1F). As breast cancer subtypes proliferate at different rates with TNBC the most proliferative tumors, followed by Her2, LB and LA tumors, we analyzed whether TIPIN expression correlated with the proliferative status of the tumors. TIPIN mRNA levels were positively correlated with Ki67, used as a proliferation marker, in the entire BC population and also within the TNBC subtype (Figure 1G). However, this link with proliferation was much weaker when we analyzed TIPIN at a protein level in the entire BC population, and was not observed within the TNBC subtype (Figure 1H). In addition, there is no difference of TIPIN protein expression between TNBC, Her2 and LB tumors (Figure 1C), although TNBC are the most proliferative tumors, followed by Her2 and then by LB tumors. These results indicate that TIPIN protein expression does not simply reflect the proliferative status of the tumors.

In conclusion, these results indicate that TIPIN is expressed at higher levels in the more aggressive BC tumors, including TNBC.

3.2. The depletion of TIPIN decreases the proliferation of BC cells

As TIPIN is known to be involved in DNA replication, we investigated the effect of its depletion on the viability of BC cells. We first confirmed that TIPIN and TIM were expressed in a large panel of established cell lines derived from human breast epithelial tissues (Supplementary Figure 3A–B). By contrast to our findings for tumors, we found no evidence of differential TIPIN RNA expression between the subtypes of human breast epithelial cell lines (Supplementary Figure 3A–B), probably due to their proliferative nature when cultured *in vitro*. Therefore, this absence of differential TIPIN expression in these proliferative BC cells is not surprising, considering the known function of TIPIN in DNA replication, and the correlation we noticed between TIPIN RNA and proliferation in tumors (Figure 1G). Interestingly, when grown in a more physiological context, in 3D culture in Matrigel (Lee et al., 2007), non-tumorigenic mammary epithelial cell lines such as MCF10A recapitulate epithelial morphogenesis by forming acinar structures (Kenny et al., 2007). In contrast, TNBC cell lines such as MDA-MB-468 exhibit disorganized structures (Kenny et al., 2007). MCF10A cells form acini within 10 days of culture and then stop to grow once these structures are formed, whereas the cancerous cells continue to

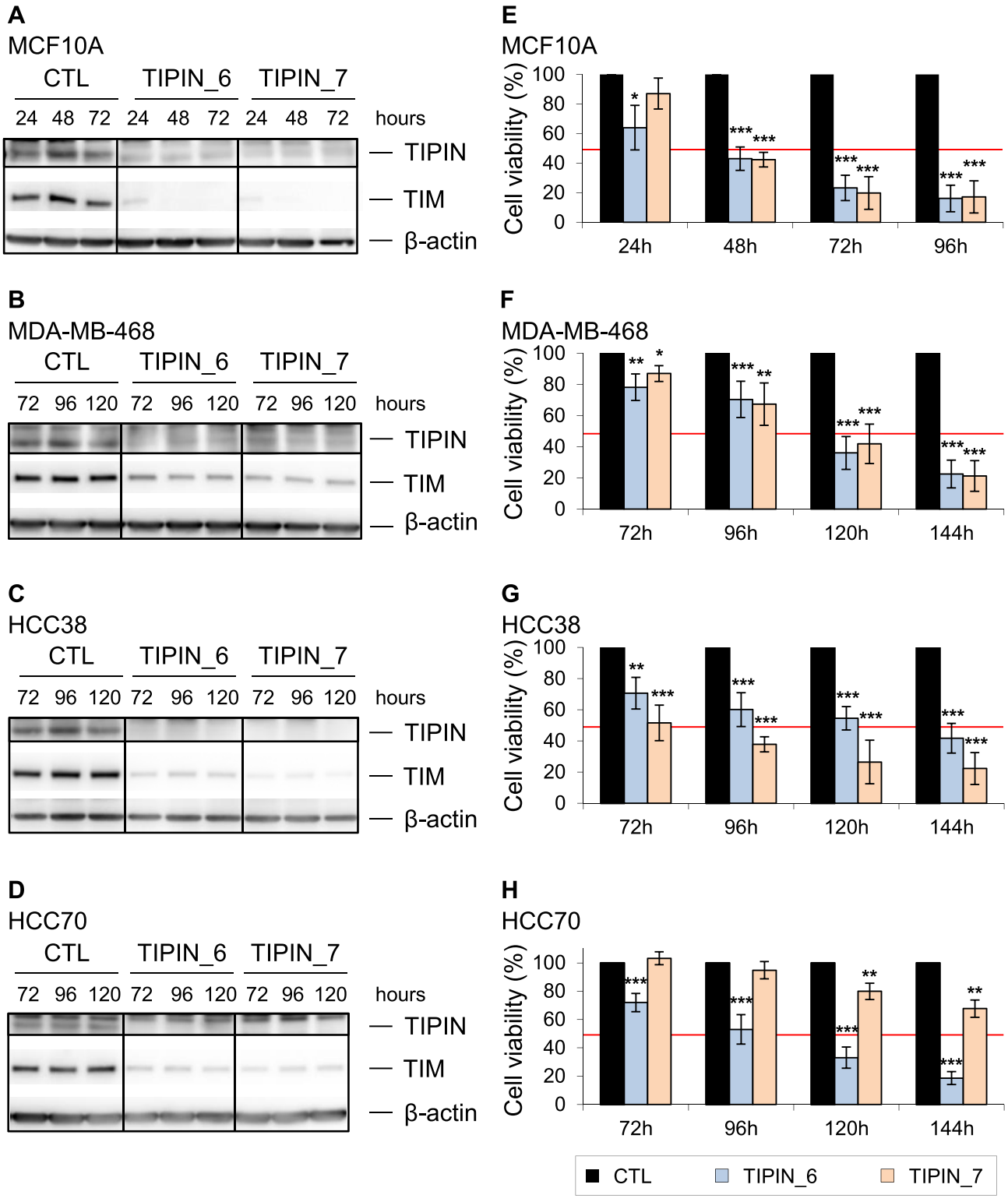

Figure 2 – The growth of breast cancer cells is impaired by TIPIN depletion. We transfected non-malignant MCF10A cells (A, E) and TNBC cell lines, MDA-MB-468 (B, F), HCC38 (C, G) and HCC70 (D, H), with a control siRNA (CTL, black bars) or two different TIPIN siRNAs TIPIN_6 (blue bars) and TIPIN_7 (orange bars). (A–D) We confirmed by immunoblotting (IB) the efficiency of TIPIN depletion. The TIPIN antibody gave additional non-specific signals (upper bands). We used β-actin as a loading control. (E–H) We analyzed cell proliferation by MTT or WST-1 assays. The error bars represent the standard deviation (SD). The p values are indicated as in Figure 1.

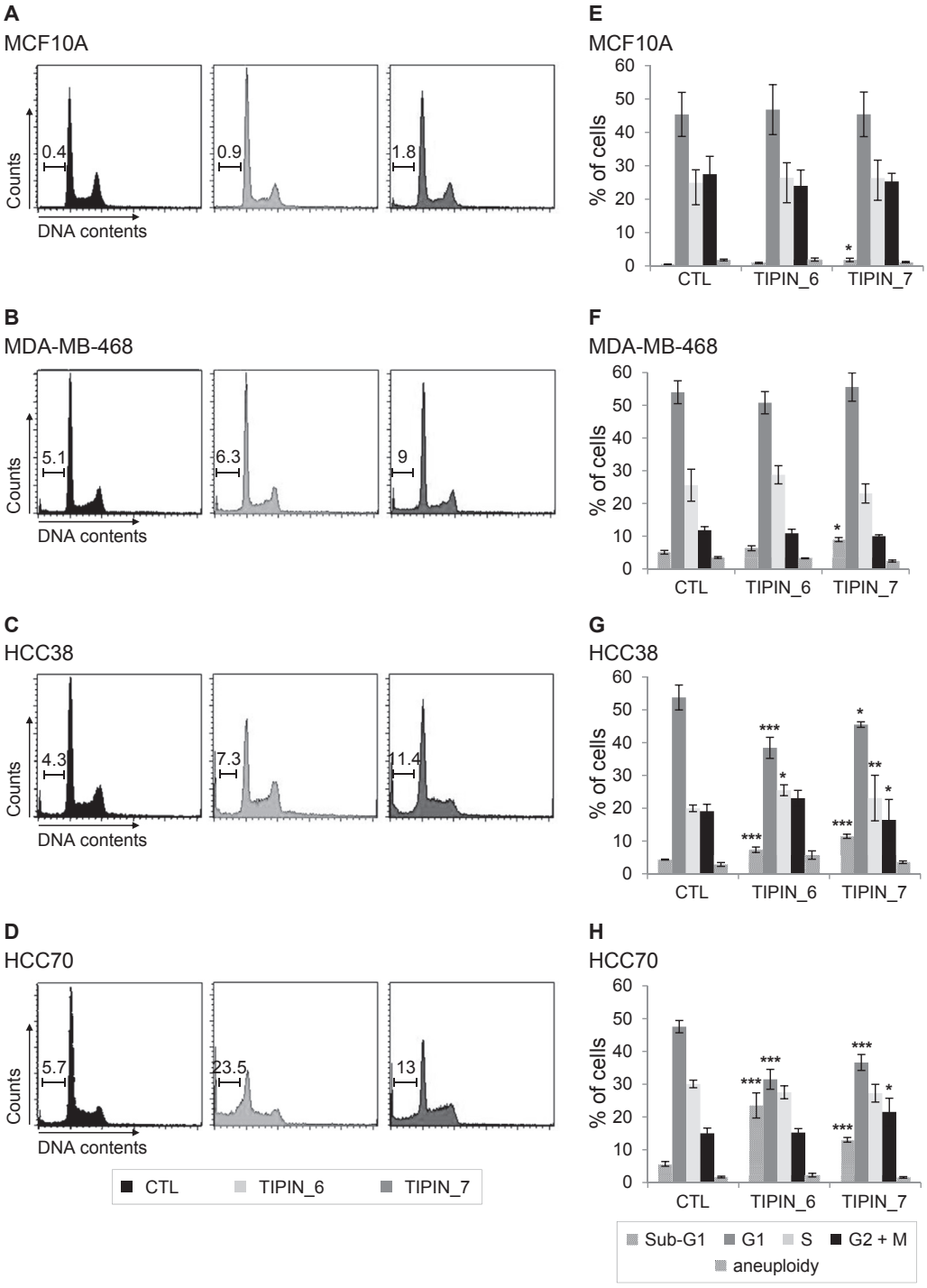

Figure 3 – TIPIN depletion affects cell cycle progression in TNBC cells. (A–D) We monitored the cell cycle status of siRNA-transfected MCF10A (A), MDA-MB-468 (B), HCC38 (C) and HCC70 (D) cells by FACs analysis following PI staining. The percentage of sub-G1 cells is indicated. (E–H) We quantified the percentage of cells within the different cell cycle phases. SD and p values are as in Figure 2.

proliferate. In these conditions, MCF10A did not express TIPIN once the acini were formed, while MDA-MB-468 cells continued to express TIPIN (Supplementary Figure 3C).

We selected three TNBC cell lines (HCC38, HCC70 and MDA-MB-468) and the non-malignant, but highly proliferative when cultured in two-dimensional (2D) onto plastic, breast cell line MCF10A for further studies.

Then, we depleted the cells of TIPIN with two different siRNAs. We confirmed that TIPIN was depleted, both at the RNA level, by quantitative RT-PCR (data not shown), and at the protein level, by immunoblotting (IB) (Figure 2A–D). Consistent with previous data (Chou and Elledge, 2006; Yoshizawa-Sugata and Masai, 2007), TIPIN depletion led to lower levels of TIM (Figure 2A–D).

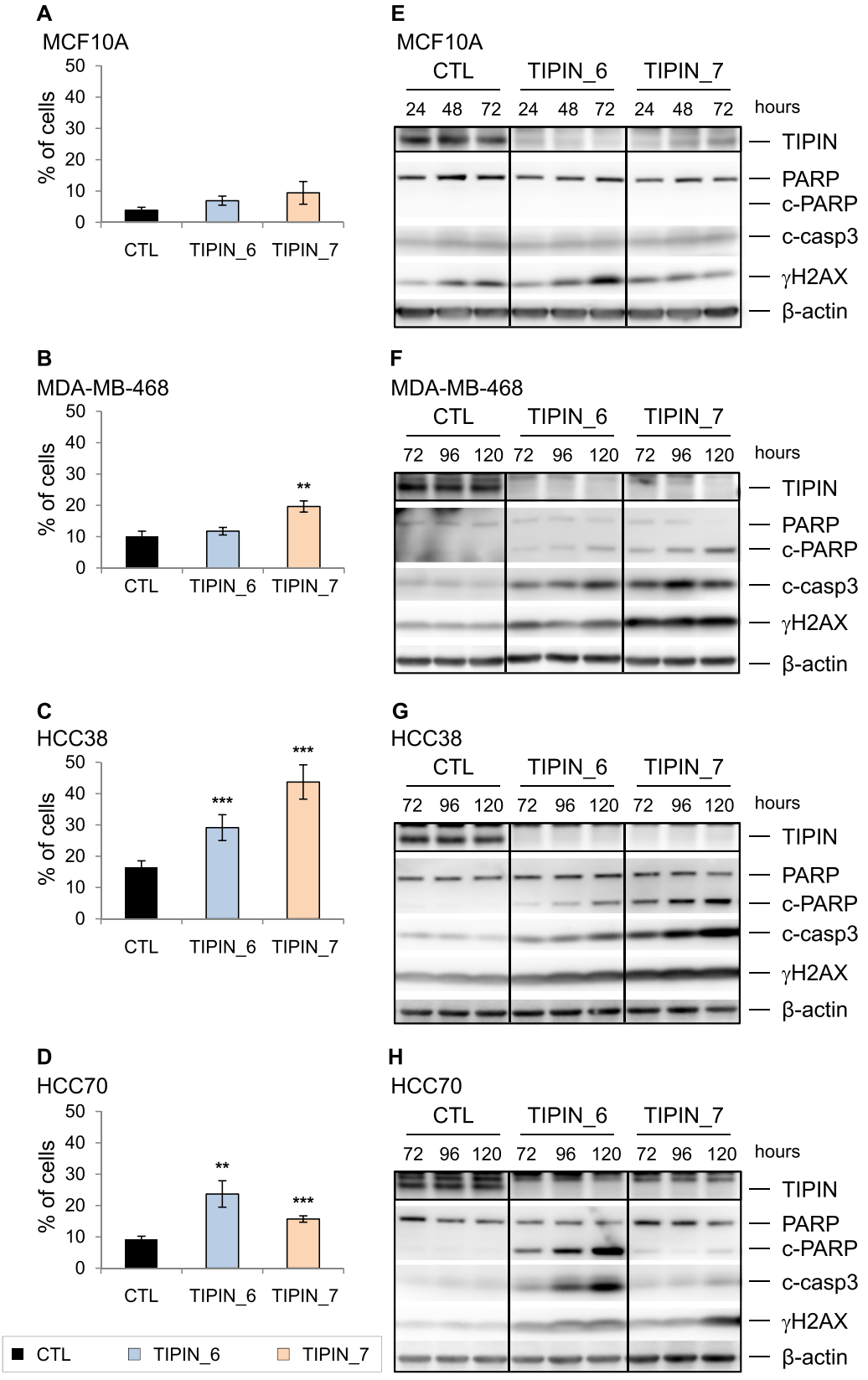

Figure 4 – Induction of apoptosis upon TIPIN depletion in BC cells. We transfected MCF10A (A, E), MDA-MB-468 (B, F), HCC38 (C, G) and HCC70 (D, H) cells with the indicated siRNAs. (A–D) We determined the percentage of apoptotic cells after PI and annexin V staining. SD and p values are as Figure 2. (E–H) We performed IB with antibodies against cleaved PARP (c-PARP), cleaved caspase 3 (c-casp3) and γH2AX. The depletion was confirmed by using an anti-TIPIN antibody. β-actin was used as a loading control.

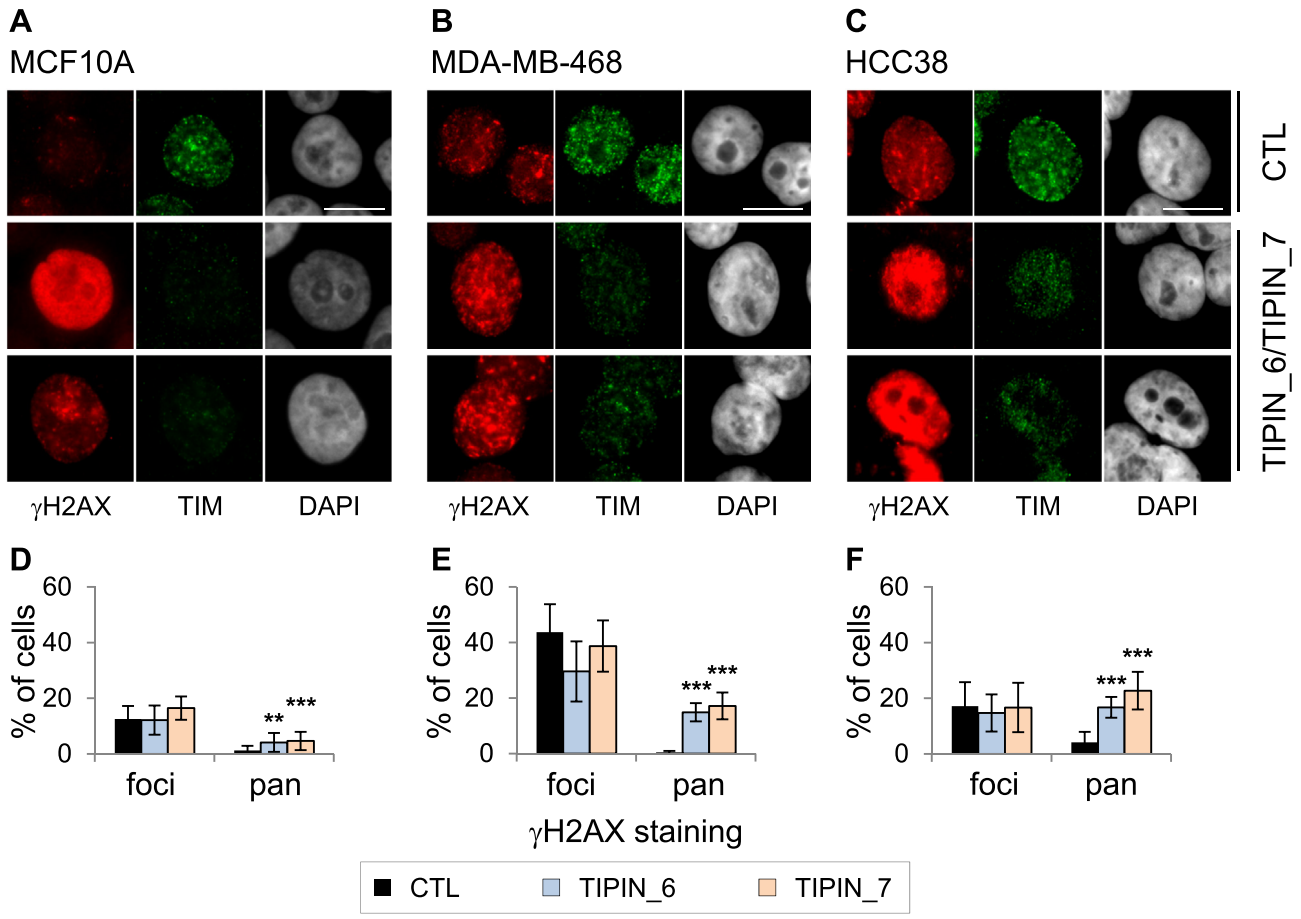

Figure 5 – Greater H2AX phosphorylation in TIPIN-depleted BC cells. We transfected MCF10A cells (A, D), MDA-MB-468 (B, E) and HCC38 (C, F) cells with the indicated siRNAs and performed immunofluorescence. (A–C) We coimmunostained the cells with anti-TIM and anti-γH2AX antibodies. We stained DNA with DAPI. The bars represent 10 μm. (D–F) We determined the percentage of cells showing at least five γH2AX foci (foci) or pan-nuclear γH2AX (pan) staining. The SD and p values are as in Figure 2.

TIPIN depletion impaired the growth of the MCF10A cells (Figure 2E) and the three TNBC cell lines (Figure 2E–H) grown in 2D onto plastic. This effect occurred earlier (24 h) in MCF10A cells than in TNBC cell lines. This time lag may be accounted for by the faster growth of MCF10A cells than of the other cell lines, with a larger number of cell divisions occurring at the time points analyzed. Indeed, the doubling times of the cell lines in 96-well plates were as follows when cultured on plastic: MCF10A (16 h), MDA-MB-468 (40 h), HCC38 (60 h) and HCC70 (50 h) (data not shown). Therefore, these data are in agreement with the function of TIPIN in DNA replication and S phase progression. Moreover, the inhibition of proliferation mediated by TIPIN depletion was not restricted to TNBC cells, but also occurred in luminal/Her2 BC cell lines: MDA-MB-453, T47D and SKBR3 (Supplementary Figure 4a–C). In conclusion, the depletion of TIPIN impairs the proliferation of breast cells.

3.3. *TIPIN depletion affects cell cycle progression in BC cells*

We then investigated the implication of TIPIN in cell cycle progression. As MCF10A cells grew much faster than the TNBC cell lines, we analyzed cell cycle profiles 48 h post-transfection for MCF10A cells and 96 h post-transfection for TNBC cells. Whereas TIPIN depletion decreased the proliferation of MCF10A cells by 60% (Figure 2E), it had no effect on their progression through the cell cycle (Figure 3A, E). This may indicate a longer cell cycle duration in MCF10A cells. By contrast, TIPIN depletion significantly decreased the G1 phase cell population and led to a flattened G2/M phase in TNBC cells (Figure 3B–D, F–H), particularly in HCC38 and HCC70 cells. In addition, the sub-G1 population, potentially corresponding to apoptotic cells, increased in size in all TIPIN-depleted TNBC cells (Figure 3B–D). The magnitude of the effects of TIPIN depletion on cell cycle progression in TNBC cells reflected the degree of cell proliferation impairment (Figure 2F–H).

3.4. *TIPIN depletion induces apoptosis in BC cells*

We performed additional experiments to determine whether TIPIN knockdown led to apoptosis in TNBC cells. For the reasons explained above, we assessed apoptosis induction 48 h and 96 h post-transfection for MCF10A and TNBC cells, respectively. Staining with annexin V confirmed that TIPIN depletion induced apoptosis in TNBC and not in MCF10A cells (Figure 4A–D). Similar results were obtained when we

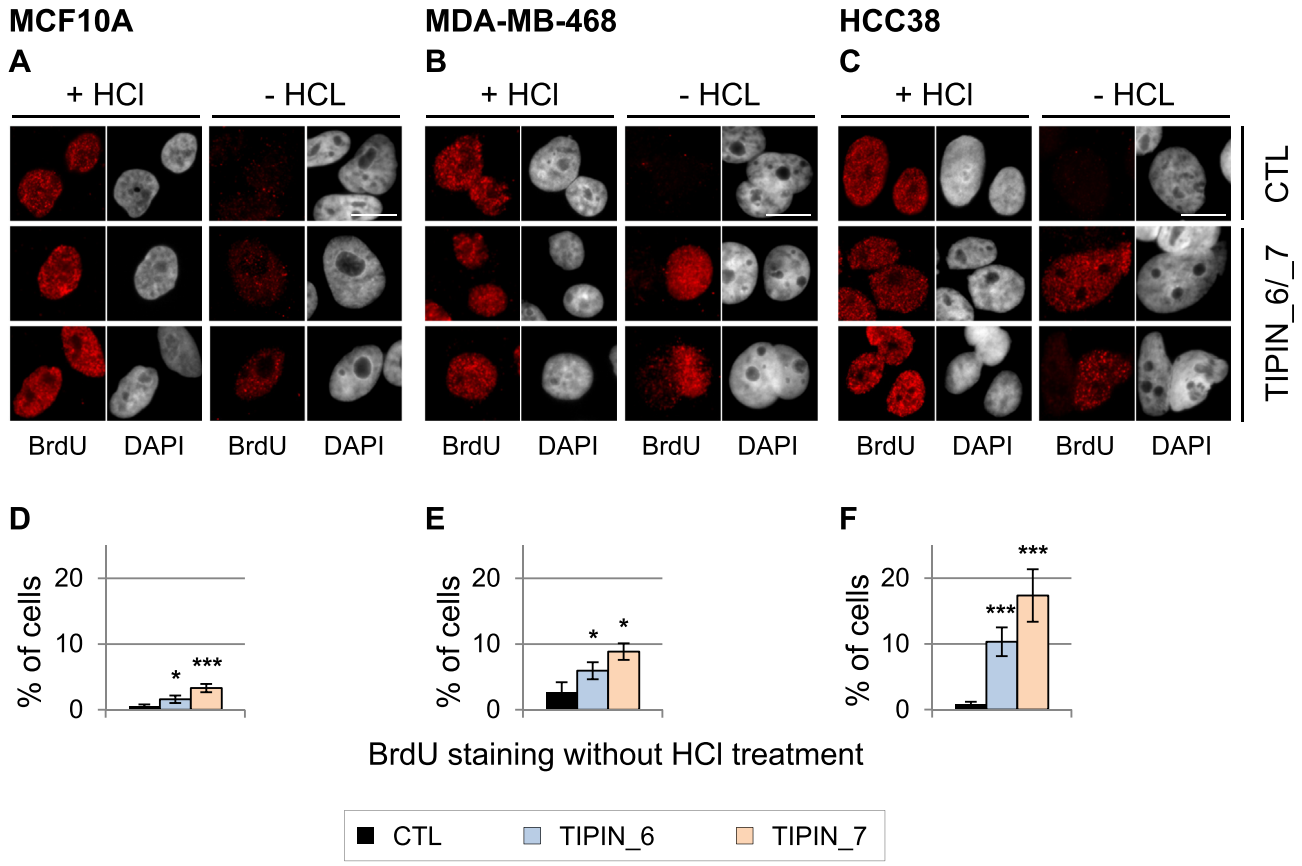

Figure 6 – TIPIN depletion leads to ssDNA formation. We transfected MCF10A cells (A, D), MDA-MB-468 (B, E) and HCC38 (C, F) cells with the indicated siRNAs and performed immunofluorescence. (A–C) The DNA of fixed cells was denatured (+HCl) or left undenatured (-HCl) before staining with an anti-BrdU antibody. The DNA was stained with DAPI. The bar represents 10 μm. (D–F) We evaluated the percentage of cells with BrdU staining in the absence of HCl denaturation. The SD and p values are as in Figure 2.

analyzed the levels of cleaved PARP and caspase 3 by IB (Figure 4E–H). Again stronger effects were observed in HCC38 and HCC70 cells (Figure 4C–D). We also examined by IB whether TIPIN depletion led to apoptosis in luminal/Her2 BC cell lines. The cleavage of caspase 3 and PARP was not detected in MDA-MB-453 cells. However, the cleaved forms of caspase 3 and PARP were observed with one siRNA in T47D cells and with the two siRNAs in SKBR3 cells (Supplementary Figure 4e–F). Altogether, our data suggest that TIPIN silencing impairs proliferation both of non-tumorigenic and cancer cells, while it may lead to apoptosis only in BC cells.

3.5. *TIPIN depletion induces higher levels of γH2AX*

IB revealed that TIPIN depletion was associated with an increase in phosphorylated histone H2AX (γH2AX) (Figure 4E–H), consistent with previous findings (Chou and Elledge, 2006). This phenomenon was more pronounced in TNBC cells than in MCF10A cells. We thus investigated the immunostaining pattern of γH2AX in TIPIN-depleted cells. We excluded HCC70 cells from the immunofluorescence (IF) experiments, because these cells tend to grow on top of each other. We fixed MCF10A and TNBC cells 48 h and 96 post-transfection, respectively, to ensure that the cells were not undergoing apoptosis (Figures 3–4). We checked the efficiency of TIPIN depletion by using an anti-TIM antibody (Figure 5A–C). As observed with PCNA or RPA staining (Supplementary Figure 5), TIM was located in characteristic nuclear foci, corresponding to sites of ongoing DNA replication, in control siRNA-transfected cells (Figure 5A–C, upper panels).

We observed two γH2AX patterns (Figure 5A–C): (i) nuclear foci and (ii) homogeneous nuclear staining (pan-nuclear). γH2AX foci are usually indicative of the presence of DNA double-strand breaks (DSBs) (Rogakou et al., 1999). The pan-nuclear γH2AX may reflect the presence of replicative stress (RS) (Toledo et al., 2008), DNA breaks (Meyer et al., 2013) or a pre-apoptotic signal (de Feraudy et al., 2010). γH2AX foci were present in 44% of MDA-MB-468 (Figure 5E), 17% of HCC38 (Figure 5F) and in 13% of MCF10A cells (Figure 5D), following transfection with control siRNA. In these control conditions, pan-nuclear γH2AX was observed in 4% of HCC38 cells and was not found in MCF10A and MDA-MB-468 cells (Figure 5D–F). Therefore, we confirmed that TNBC cells, at a steady-state level, displayed more γH2AX staining than MCF10A cells. TIPIN depletion increased the number of cells with pan-nuclear γH2AX, but not with γH2AX foci (Figure 5D–F).

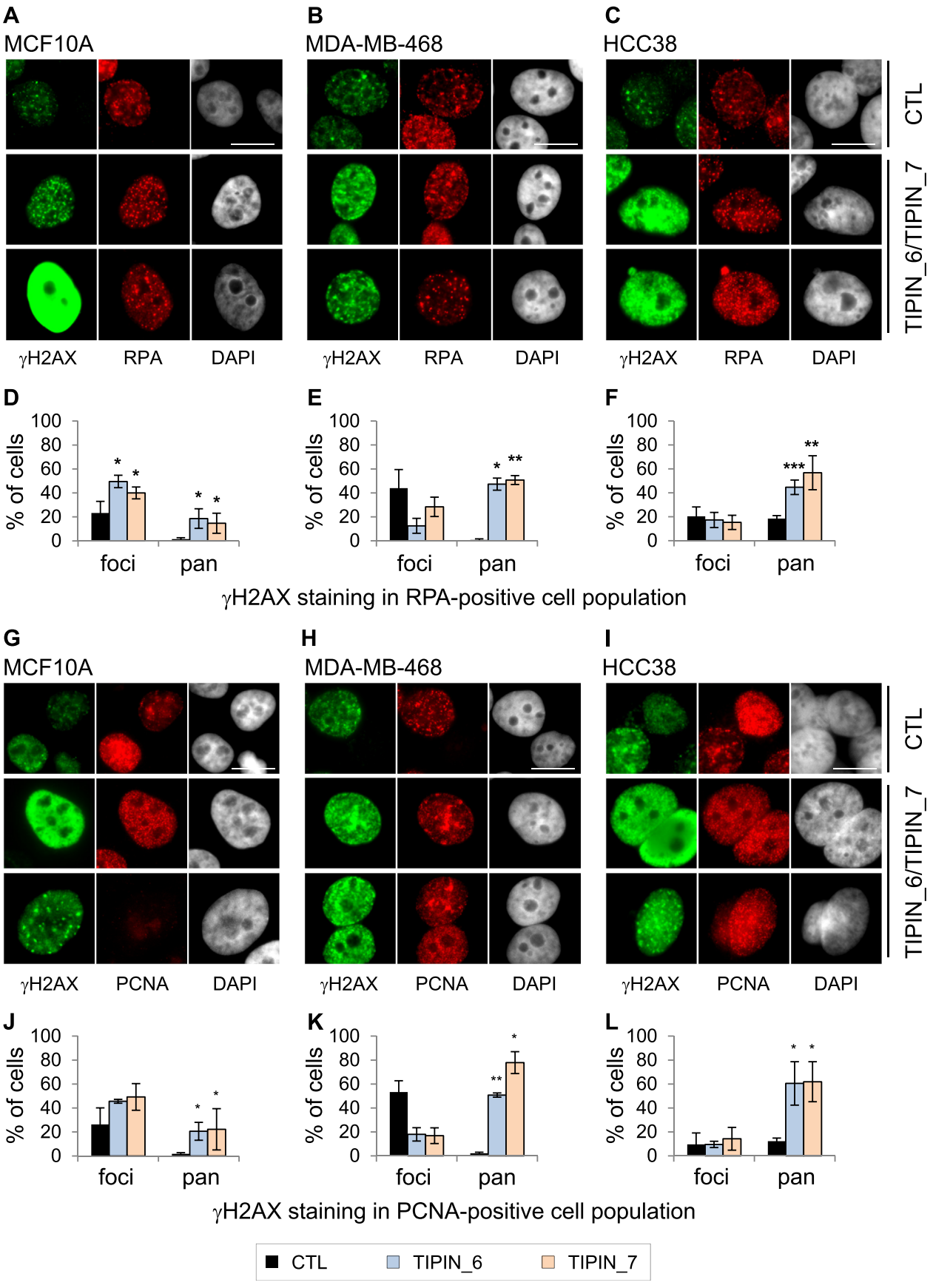

Figure 7 – Pan-nuclear staining occurs in S phase in TIPIN-depleted BC cells. We treated non-tumorigenic MCF10A cells (A, D, G and J), and MDA-MB-468 (B, E, H and K) and HCC38 (C, F, I and L) TNBC cells as in Figure 5 and performed immunofluorescence. (A-C and G-I) The

3.6. TIPIN depletion causes increased replicative stress in BC cells

We investigated whether the pan-nuclear γH2AX observed following TIPIN depletion resulted from RS, which can be visualized by the presence of ssDNA (Aguilera and Garcia-Muse, 2013; Tourriere and Pasero, 2007). After siRNA transfection, cells were grown in the presence of BrdU, for 48 h for MCF10A cells and 72 h for TNBC cells. We verified by DNA denaturation that BrdU was incorporated into the whole genome (Figure 6A–C, panels + HCl). Without denaturation (Raderschall et al., 1999), the anti-BrdU antibody has access to its epitope only in long regions (patches) of ssDNA within the genome (Figure 6A–C, panels -HCl). Few control siRNA-transfected cells displayed such patches of ssDNA (Figure 6D–F). Upon TIPIN depletion, BrdU staining was found only in discrete foci in 2–3% of MCF10A cells (Figure 6A,D), but throughout the whole nucleus in 6–8% of MDA-MB-468 and 10–17% of HCC38 cells (Figure 6B–C,E-F). This indicated higher levels of ssDNA in TIPIN-depleted cells compared to MCF10A cells.

To confirm that pan-nuclear γH2AX upon TIPIN silencing is linked to RS, we analyzed the γH2AX staining during replication by performing co-staining with anti-RPA or anti-PCNA antibodies. The number of RPA- or PCNA-positive BC cells was unaffected by TIPIN depletion (Figure 7A–C,G-I and data not shown), consistent with the absence of S phase arrest (Figure 3). However, pan-nuclear γH2AX was detected in more than 50% of RPA-positive and 60% of PCNA-positive TIPIN-depleted TNBC cells (Figure 7E–F,K-L), but in only 17% of RPA-positive and 20% of PCNA-positive TIPIN-depleted MCF10A cells (Figure 7D,J). Thus, pan-nuclear γH2AX could be related to the formation of ssDNA in TIPIN-depleted TNBC cells during S phase.

In conclusion, the high levels of pan-nuclear γH2AX in TIPIN-depleted TNBC cells suggest that these cells were unable to resolve patches of ssDNA (Figures 5–7), underlying DNA replication defects.

3.7. TIPIN depletion slows the progression of DNA replication forks

These findings led us to explore replication in more details in TIPIN-depleted cells by performing DNA combing experiments (Anglana et al., 2003; Techer et al., 2013) (Figure 8A–B). MDA-MB-468 and HCC38 cells, unlike MCF10A, spontaneously displayed fork asymmetry, as demonstrated by the unequal lengths of the IdU and CldU tracks (Figure 8C), highlighting abnormal fork progression and thus the presence of RS.

TIPIN depletion significantly decreased median fork speed in all BC cells (Figure 8D–F). The inter-origin (IOD) and inter-termination (ITD) distances were significantly shorter in TIPIN-depleted MCF10A, but not in TIPIN-depleted TNBC cells (Figure 8G–I). These results suggest that TIPIN-depleted MCF10A cells respond to the slower progression of the replication fork by firing dormant origins. This may account for the decreased cell proliferation in TIPIN-silenced MCF10A cells (Figure 2E) in the absence of an effect on cell cycle distribution (Figure 3A). By contrast, TIPIN-depleted TNBC cells were unable to activate dormant origins, as demonstrated by the lack of change in IOD and ITD (Figure 8H–I). They underwent apoptosis, probably because they were unable to resume replication.

3.8. TIPIN depletion decreases tumorigenicity and delays tumor growth

To evaluate the potential therapeutic value of targeting TIPIN, we investigated the effect of TIPIN silencing on the tumorigenic properties of TNBC cells through the anchorage-independent assay of colony formation in soft agar (Figure 9A–B). We excluded HCC38 and MCF10A cells from this assay because they do not form colonies in semi-solid medium. TIPIN-depleted MDA-MB-468 and HCC70 cells displayed an impairment of colony formation in soft-agar (Figure 9A–B).

We next evaluated the effects of TIPIN knockdown on tumor growth *in vivo*, by inoculating immunodeficient mice with the same amount of viable MDA-MB-468 cells that had been transfected the day before with control or TIPIN siRNAs (Figure 9D). Tumor growth was significantly delayed in animals injected with TIPIN-depleted cells than in animals receiving control siRNA-transfected cells (Figure 9C).

Together these assays indicate that TIPIN plays an important role in the malignancy of TNBC cells, suggesting that TIPIN may be a useful potential target for the treatment of TNBC tumors.

4. Discussion

In the absence of targeted therapies, patients with TNBC are currently treated exclusively by conventional cytotoxic chemotherapy. These tumors respond well to such treatment initially, but they relapse more frequently than tumors from other BC subgroups and are responsible for a disproportionate number of BC deaths. The identification of relevant therapeutic targets for the treatment of TNBC patients remains a critical issue for improving the survival of such patients. We therefore searched for proteins involved in replication fork protection and displaying overexpression in human TNBC biopsies. We found that TIPIN mRNA levels were very high in TNBC samples, despite these tumors having a lower CN for *TIPIN*. At the protein level, we observed that both TIPIN and TIM were higher expressed in the most proliferative and poor prognosis associated BC subtypes (TNBC, Her2, LB) compared to the low proliferative and good prognosis associated LA tumors. Other studies have shown that TIPIN and TIM are under-expressed in kidney (Mazzoccoli et al., 2012) and pancreatic (Relles et al., 2013) cancers. By contrast, TIM is overexpressed in bladder (Schepeler et al., 2013) and lung (Yoshida et al., 2013) cancers. We found that the levels of TIPIN mRNA and the proliferation marker Ki67 were strongly

cells were fixed and immunostained with anti-γH2AX and anti-RPA (A–C) or anti-PCNA (G–I) antibodies. The DNA was stained with DAPI. The bar represents 10 μm. (D-F and J-L) We quantified the percentage of RPA-positive (D–F) and PCNA-positive (J–L) cells displaying γH2AX (foci or pan) staining. The SD and p values are as in Figure 2.

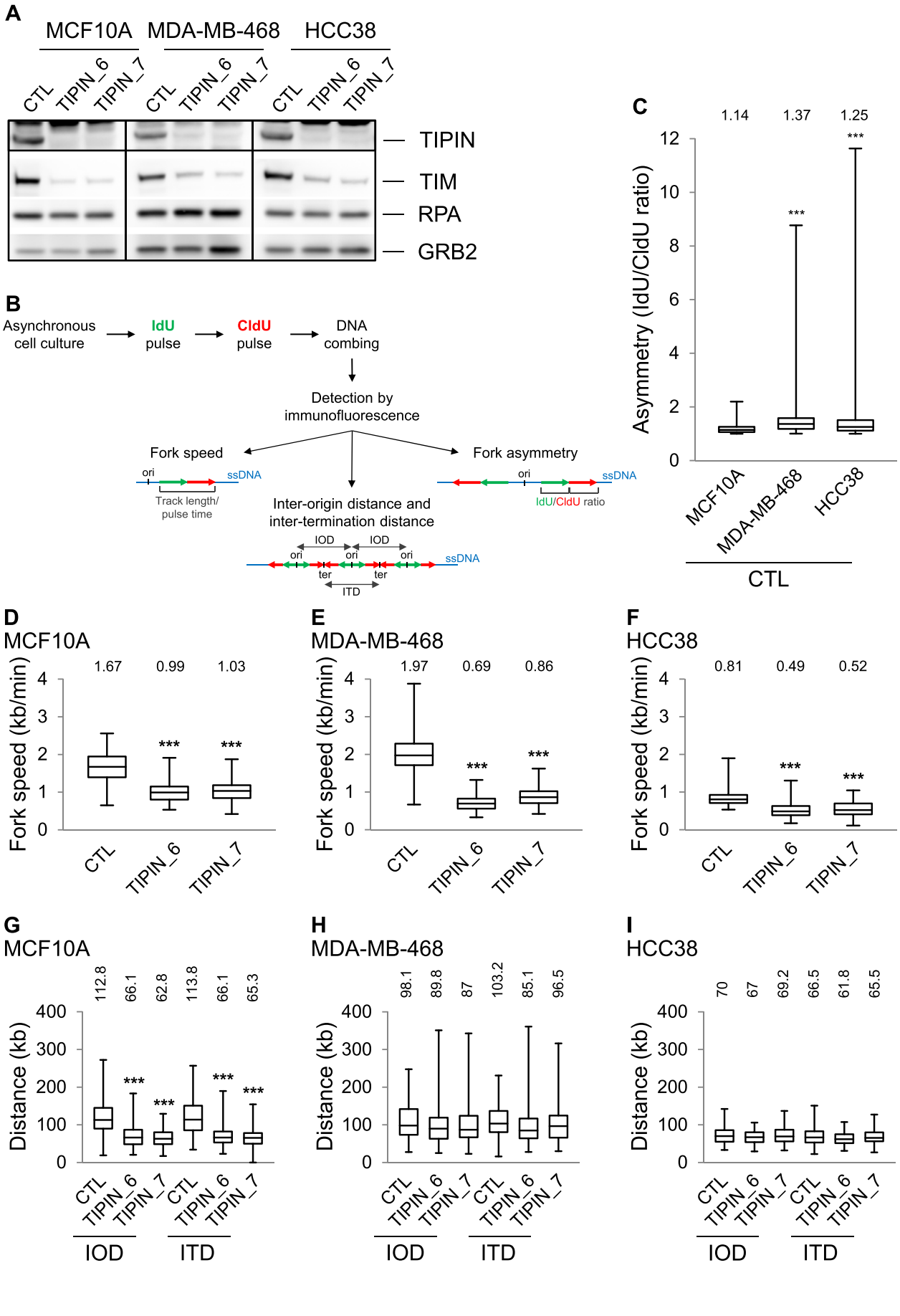
A
MCF10A
MDA-MB-468
HCC38
CTL
TIPIN_6
TIPIN_7
TIPIN
TIM
RPA
GRB2
B
Asynchronous cell culture
IdU pulse
CldU pulse
DNA combing
Detection by immunofluorescence
Fork speed
Track length/ pulse time
Fork asymmetry
IdU/CldU ratio
Inter-origin distance and inter-termination distance
IOD
ori
ter
ITD
ssDNA
C
Asymmetry (IdU/CldU ratio)
1.14
1.37
1.25
MCF10A
MDA-MB-468
HCC38
CTL
D
MCF10A
Fork speed (kb/min)
1.67
0.99
1.03
E
MDA-MB-468
1.97
0.69
0.86
F
HCC38
0.81
0.49
0.52
G
MCF10A
Distance (kb)
112.8
66.1
62.8
113.8
66.1
65.3
IOD
ITD
H
MDA-MB-468
98.1
89.8
87
103.2
85.1
96.5
I
HCC38
70
67
69.2
66.5
61.8
65.5

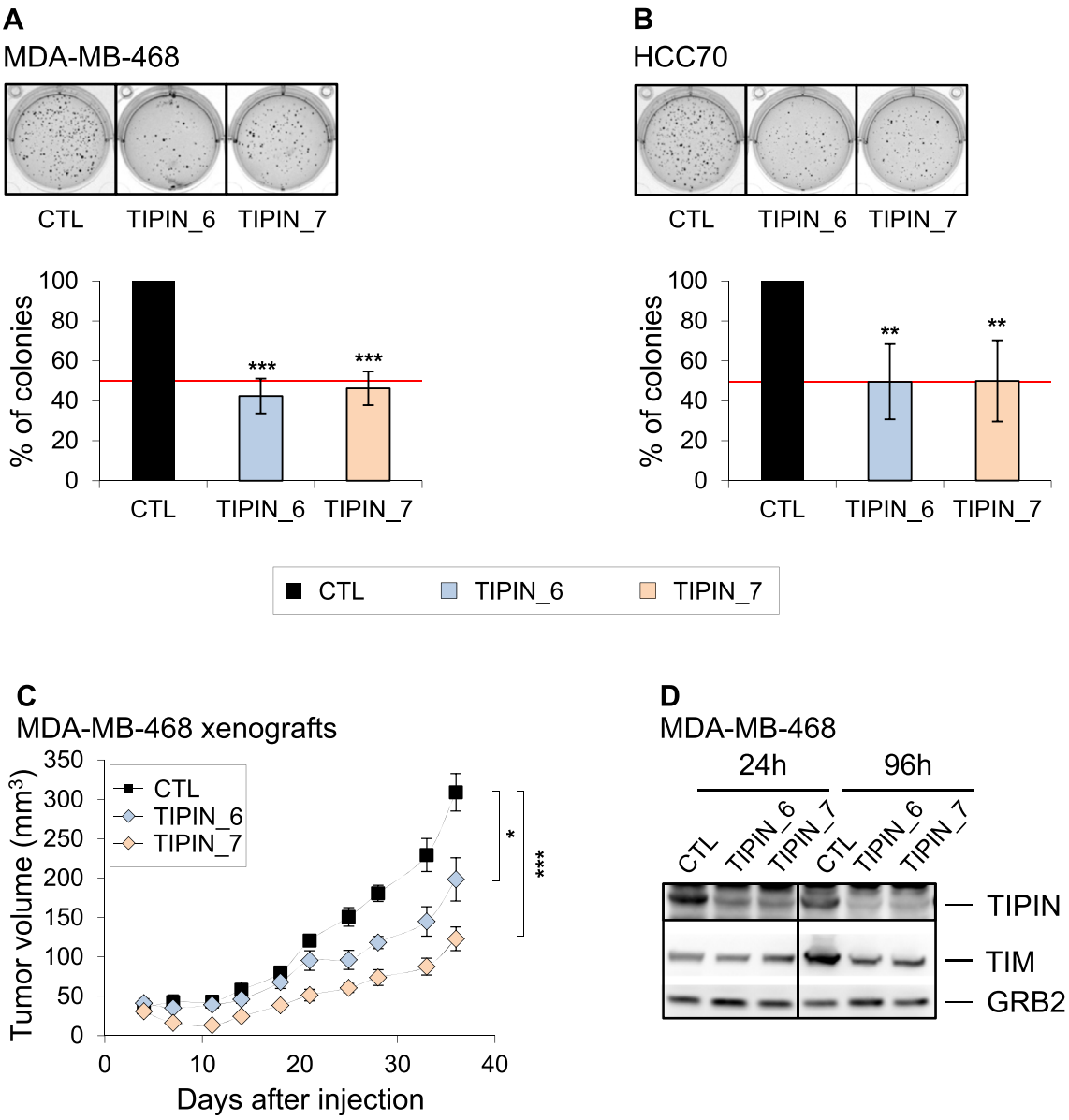

Figure 9 – TIPIN depletion decreases tumorigenicity *in vitro* and tumor growth *in vivo*. (A–B) We transfected MDA-MB-468 (A) and HCC70 (B) cells with the indicated siRNAs. We grow them in soft agar (top panels). We stained and counted colonies (bottom panels). (C–D) We transfected MDA-MB-468 cells with the indicated siRNAs and injected 24 h later the same number of viable cells subcutaneously into five Swiss *nude* mice per siRNA-related group. We evaluated tumor growth twice weekly (C). We checked the efficiency of depletion by IB (D) with antibodies against TIPIN and TIM. We used GRB2 as a loading control. The SD and p values are as in Figure 2.

positively correlated ($p < 2.2 \times 10^{-16}$ in the entire population; $p = 0.008$ in TNBC). However, this link between TIPIN and proliferation was much weaker or inexistent when we analyzed TIPIN at the protein level ($p = 0.02$ in the entire population; $p = 0.66$ in TNBC). This is in agreement with the fact that there is no difference of TIPIN protein expression between TNBC, Her2 and LB tumors, in spite of TNBC are the most proliferative tumors, followed by Her2 and then by LB tumors. These results indicate that TIPIN protein expression does not simply reflect the proliferative status of the tumors.

Figure 8 – TIPIN depletion slows the progression of DNA replication. We transfected MCF10A cells (A, D, G), MDA-MB-468 (A, E, H) and HCC38 (A, F, I) cells with the indicated siRNAs. Then we pulse-labeled cells with IdU and CldU for 30 min and performed DNA combing. (A) We confirmed the efficiency of TIPIN depletion by IB with antibodies against TIPIN and TIM. We used GRB2 as a loading control. (B) Scheme of single-molecule analysis of DNA replication. IdU tracks are shown in green, CldU tracks in red and ssDNA in blue. (C) Boxplots show the distribution of the ratio of the lengths of IdU and CldU tracks on combed DNA for the CTL siRNA-transfected cells. (D–I) Boxplots show the distribution of replication fork speed (D–F) and the distribution of the inter-origin (IOD) and inter-termination (ITD) distances (G–I). We indicated the SD by error bars and the p values for Mann–Whitney test by asterisks (*$p < 0.001$).**

We investigated the potentially deleterious effect of TIPIN silencing on BC cell lines. Consistent with the findings of other studies (Chou and Elledge, 2006; Yoshizawa-Sugata and Masai, 2007), we found that the siRNA-mediated depletion of TIPIN compromised cell proliferation in the non-tumorigenic cell line examined (MCF10A) and in BC cells. TIPIN-depleted MCF10A cells compensated for the slower DNA replication fork speed by firing latent replication origins. However, this compensation may be not sufficient, resulting in lower rates of cell proliferation, consistent with previous findings (Chou and Elledge, 2006; Gotter et al., 2007; Unsal-Kacmaz et al., 2007; Yoshizawa-Sugata and Masai, 2007). Despite this effect on proliferation, TIPIN silencing did not induce apoptosis and had no effect on cell cycle progression in MCF10A cells. Previous papers showed contradictory results in TIPIN-depleted cells, as some cells displayed normal (Smith et al., 2009) or abnormal (Smith-Roe et al., 2013; Yoshizawa-Sugata and Masai, 2007) cell cycle progression. We did not find an arrest in G2 phase in TIPIN-depleted MCF10A cells, in contrast to TIPIN-depleted fibroblasts (Smith-Roe et al., 2013). This discrepancy may be explained by the nature of the "normal" cells analyzed: epithelial cells vs fibroblast cells. By contrast to non-cancerous MCF10A cells, TIPIN-depleted BC cells displayed higher levels of apoptosis, as revealed by the large sub-G1 cell population and the high number of annexin-V positive cells, together with the induction of caspase 3/7 activities and PARP cleavage. Together, our data therefore suggest that TIPIN depletion may selectively impair the viability of breast tumor cells. However, analysis of TIPIN depletion in additional "normal" mammary epithelial cells should be performed to strengthen this conclusion.

As the TIPIN-TIM complex is involved in DNA replication fork stability, we investigated the mechanisms driving BC cells to undergo apoptosis upon TIPIN depletion. We found that TIPIN silencing led to ssDNA formation and H2AX phosphorylation, as shown in previous studies (Chou and Elledge, 2006; Smith et al., 2009), together with an increase in the chromatin-bound fraction of RPA, which was stronger in BC cells. Thus, TIPIN depletion leads to RS, consistent with the role of TIPIN-TIM complex in the coupling of the DNA helicase to the polymerase to prevent excessive DNA unwinding (Gotter et al., 2007). Moreover, increased γH2AX was observed specifically in S phase in both TIPIN-depleted MCF10A and TNBC cells, whereas pan-nuclear γH2AX was found only in TNBC cells. As γH2AX is not a specific marker of RS, we assume that this staining corresponds to DSBs resulting from fork collapse (Branzei and Foiani, 2010) or represents a pre-apoptotic signal, as recently reported (de Feraudy et al., 2010). In MCF10A and BC cells, TIPIN depletion reduces DNA replication fork speed, revealing increased RS, in agreement with previous reports (Smith-Roe et al., 2013; Smith et al., 2009; Yoshizawa-Sugata and Masai, 2007). In response to slower replication fork progression, TIPIN-depleted MCF10A cells react by firing dormant replication origins, partly compensating for this slowing and, presumably, ensuring replication resumption and termination before the cell enters in mitosis. The activation of dormant replication origins is an essential phenomenon allowing cancer cells to survive RS (Ge et al., 2007). In contrast to MCF10A cells, TNBC cells display spontaneous RS, as revealed by the significant increase in asymmetry of sister forks, reflecting perturbed fork progression (Techer et al., 2013). These cells are unable to activate dormant origins in the absence of TIPIN, because IOD and ITD are no lower than in CTL-transfected TNBC cells, probably because they have been already utilized and therefore unavailable. This may result in under replicated DNA, leading to a massive pan-nuclear distribution of γH2AX and apoptosis. Thus, TIPIN appears to be essential for the survival of genetically unstable cells subjected to chronic RS.

TIPIN is not crucial for DNA replication (Unsal-Kacmaz et al., 2007), so why are TIPIN-depleted TNBC cells unable to sustain DNA replication? Like TNBC tumors, in which the *TP53* gene is frequently mutated, the three TNBC cell lines used in this study were p53-deficient (Holstege et al., 2009; Manie et al., 2009; Shah et al., 2012). CHK1 and ATR inhibitors have been shown to generate DNA lesions in S phase, and such lesions are particularly toxic in p53-deficient cells (Reaper et al., 2011; Toledo et al., 2011). The severe phenotypes observed in TIPIN-depleted TNBC cells may therefore be due to their p53 deficiency. Alternatively, homologous recombination (HR) in TNBC may be impaired by *BRCA1* mutation or promoter methylation (the "BRCAness" phenotype) (Popova et al., 2012; Turner et al., 2004) or PTEN deficiency (Marty et al., 2008; Saal et al., 2008; Stemke-Hale et al., 2008). The *BRCA1* promoter is methylated in HCC38 cells (Popova et al., 2012) and PTEN protein is undetectable in MDA-MB-468 and HCC70 cells (Marty et al., 2008; Ni et al., 2012). As HR is also required to restart collapsed DNA replication forks (Aze et al., 2013), TIPIN-depleted TNBC cells may be unable to restart replication once it has stalled, due to their "BRCAness" phenotype (Schlacher et al., 2011, 2012).

In addition to the induction of apoptosis in BC cells but not in MCF10A cells, we showed that TIPIN knockdown impaired the growth of TNBC cells in soft agar and slowed tumor growth *in vivo* in xenograft models. This suggests that TIPIN may be considered as a candidate therapeutic target, in agreement with anti-tumor strategies targeting DNA replication (Ma et al., 2012; Toledo et al., 2011). Despite the high sensitivity of TNBC tumors to chemotherapy (cyclophosphamide/doxorubicin), these tumors frequently recur and TNBC patients have worse survival outcomes than patients with BC of other subtypes (Liedtke et al., 2008; Metzger-Filho et al., 2012). Both cyclophosphamide and doxorubicin interferes with DNA replication by blocking the progression of replication forks. Therefore, the targeting of TIPIN in association with this standard protocol may be beneficial to patients through additional or synergic effects, or may make it possible to decreases the doses of chemotherapy agents used, thereby minimizing adverse effects. Additional experiments will be required to test this hypothesis *in vivo* in TNBC xenograft models. Our data require confirmation in other normal cell lines, but they suggest that TIPIN depletion does not affect replication in MCF10A cells, highlighting a potentially selective effect on BC cells. In addition, we have found that TIPIN is not expressed at the protein level in MCF10A, once they form acini in a more physiological conditions (Matrigel), and stop to proliferate. Overall, our findings suggest that TIPIN may be an attractive target for the treatment of the poor prognosis associated BC such as TNBC, in which high levels of TIPIN may be required for the completion of DNA replication in a genetically

unstable context. However, we cannot exclude possible side effects in proliferative tissues, such as bone marrow or stomach.

Targeting RS could be achieved with inhibitors of protein kinases such as ATR or CHK1 as already documented by others (Abdel-Fatah et al., 2014; Bartek et al., 2012; Fokas et al., 2014; Lecona and Fernandez-Capetillo, 2014; Merry et al., 2010). In order to be more specific and to avoid potential side effects, targeting directly TIPIN, by interfering with protein–protein interactions, could be an alternative option. An approach could be the inhibition of the interaction between TIPIN and RPA. Indeed, inhibitors of the association between RPA with some of its partners have recently been described (Frank et al., 2013; Glanzer et al., 2011). Alternatively, TIPIN and TIM proteins stabilize each other (Chou and Elledge, 2006; Yoshizawa-Sugata and Masai, 2007), and we found that TIPIN depletion led to lower levels of both TIPIN and TIM, in agreement with previous report (Smith-Roe et al., 2013). Therefore, targeting TIPIN/TIM complex formation may represent a strategy to inhibit TIPIN function as well as a therapeutic approach. Noteworthy, targeting TIPIN or TIM may not lead to identical phenotypes since it has been reported that TIM has a function in sister chromatid cohesion that is independent of the TIM-TIPIN complex (Smith-Roe et al., 2011).

5. Conclusions

TNBC is a subgroup of breast cancer accounting for a disproportionate number of deaths from this disease. Treatments based on new therapeutic targets remain a critical issue for improving the survival of TNBC patients. We found that a factor involved in DNA replication fork stability, TIPIN, is overexpressed in the poor prognosis associated BC including TNBC and is essential for cell proliferation and DNA replication progression in both human BC and non-tumorigenic cells. Unlike normal cells, TNBC cells cannot fire dormant replication origins to ensure complete DNA duplication in the absence of TIPIN. Instead, they undergo apoptosis. Importantly, TIPIN is also required for TNBC cell tumorigenicity and its depletion slows tumor growth. In line with the renewal of interest in the targeting of DNA replication as a strategy for anti-tumor therapy, our findings suggest that TIPIN is a potentially attractive target for the treatment of the most proliferative and aggressive BC subtypes, including TNBC.

Conflict of interest

The authors declare on conflict of interest regarding this article.

Financial support

This work was supported by Institut de Recherches Servier and Institut Curie. LDK is supported by a grant from Cancéropôle Ile de France.

Acknowledgments

We thank Virginie Maire, Bérengère Marty-Prouvost, Dr Sylvie Maubant, Dr David Silvestre, Dr Tania Tahtouh (Dr Dubois' laboratory), Dr Philippe Pasero and Dr Hélène Tourrière (Institut de Génétique Humaine, CNRS UPR1142) and Dr Marc-Henri Stern (Institut Curie, INSERM U830) for discussions and/or critical reading of the manuscript. We are grateful to Bérengère Marty-Prouvost for providing protein lysates of cells cultured in Matrigel. We thank Dr Bernard Asselain (Institut Curie, INSERM U900), Dr Anne Vincent-Salomon (Institut Curie, Tumor Biology, Service of Pathology) and Martine Yann for their assistance in the selection of the human tumors. We thank Dr Xavier Sastre-Garau (Institut Curie, Department of Tumor Biology), his colleagues from the Biological Resource Center of Institut Curie, the patients and Dr Fabien Reyal (Institut Curie, Surgery Department and $(RT)^2$ Lab) for providing tumor samples and normal breast tissues. We thank Dr Niclas Setterblad and his colleagues for use of the FACs facilities (Plateforme Technologique, IUH, Paris 7). We thank Sandrine Carignon (Institut Curie, CNRS UMR 3244) for technical assistance for the DNA combing experiments.

Appendix A. Supplementary data

Supplementary data related to this article can be found at http://dx.doi.org/10.1016/j.molonc.2015.04.010.

REFERENCES

Abdel-Fatah, T.M., Middleton, F.K., Arora, A., Agarwal, D., Chen, T., Moseley, P.M., Perry, C., Doherty, R., Chan, S., Green, A.R., Rakha, E., Ball, G., Ellis, I.O., Curtin, N.J., Madhusudan, S., 2014. Untangling the ATR-CHEK1 network for prognostication, prediction and therapeutic target validation in breast cancer. Mol. Oncol. 9, 569–585.

Aguilera, A., Garcia-Muse, T., 2013. Causes of genome instability. Annu. Rev. Genet. 47, 1–32.

Ali, S.I., Shin, J.S., Bae, S.H., Kim, B., Choi, B.S., 2010. Replication protein A 32 interacts through a similar binding interface with TIPIN, XPA, and UNG2. Int. J. Biochem. Cell Biol. 42, 1210–1215.

Anglana, M., Apiou, F., Bensimon, A., Debatisse, M., 2003. Dynamics of DNA replication in mammalian somatic cells: nucleotide pool modulates origin choice and interorigin spacing. Cell 114, 385–394.

Aze, A., Zhou, J.C., Costa, A., Costanzo, V., 2013. DNA replication and homologous recombination factors: acting together to maintain genome stability. Chromosoma 122, 401–413.

Baldeyron, C., Soria, G., Roche, D., Cook, A.J., Almouzni, G., 2011. HP1alpha recruitment to DNA damage by p150CAF-1 promotes homologous recombination repair. J. Cell Biol. 193, 81–95.

Bartek, J., Mistrik, M., Bartkova, J., 2012. Thresholds of replication stress signaling in cancer development and treatment. Nat. Struct. Mol. Biol. 19, 5–7.

Branzei, D., Foiani, M., 2010. Maintaining genome stability at the replication fork. Nat. Rev. Mol. Cell Biol. 11, 208–219.

Cancer Genome Atlas, N., 2012. Comprehensive molecular portraits of human breast tumours. Nature 490, 61–70.

Cerqueira, A., Santamaria, D., Martinez-Pastor, B., Cuadrado, M., Fernandez-Capetillo, O., Barbacid, M., 2009. Overall Cdk activity modulates the DNA damage response in mammalian cells. J. Cell Biol. 187, 773–780.

Chang, W., Gao, X., Han, Y., Du, Y., Liu, Q., Wang, L., Tan, X., Zhang, Q., Liu, Y., Zhu, Y., Yu, Y., Fan, X., Zhang, H., Zhou, W., Wang, J., Fu, C., Cao, G., 2013. Gene expression profiling-derived immunohistochemistry signature with high prognostic value in colorectal carcinoma. Gut 63, 1457–1467.

Chou, D.M., Elledge, S.J., 2006. Tipin and timeless form a mutually protective complex required for genotoxic stress resistance and checkpoint function. Proc. Natl. Acad. Sci. U S A 103, 18143–18147.

Curtis, C., Shah, S.P., Chin, S.F., Turashvili, G., Rueda, O.M., Dunning, M.J., Speed, D., Lynch, A.G., Samarajiwa, S., Yuan, Y., Graf, S., Ha, G., Haffari, G., Bashashati, A., Russell, R., McKinney, S., Group, M., Langerod, A., Green, A., Provenzano, E., Wishart, G., Pinder, S., Watson, P., Markowetz, F., Murphy, L., Ellis, I., Purushotham, A., Borresen-Dale, A.L., Brenton, J.D., Tavare, S., Caldas, C., Aparicio, S., 2012. The genomic and transcriptomic architecture of 2,000 breast tumours reveals novel subgroups. Nature 486, 346–352.

de Feraudy, S., Revet, I., Bezrookove, V., Feeney, L., Cleaver, J.E., 2010. A minority of foci or pan-nuclear apoptotic staining of gammaH2AX in the S phase after UV damage contain DNA double-strand breaks. Proc. Natl. Acad. Sci. U S A 107, 6870–6875.

Fokas, E., Prevo, R., Hammond, E.M., Brunner, T.B., McKenna, W.G., Muschel, R.J., 2014. Targeting ATR in DNA damage response and cancer therapeutics. Cancer Treat Rev. 40, 109–117.

Frank, A.O., Feldkamp, M.D., Kennedy, J.P., Waterson, A.G., Pelz, N.F., Patrone, J.D., Vangamudi, B., Camper, D.V., Rossanese, O.W., Chazin, W.J., Fesik, S.W., 2013. Discovery of a potent inhibitor of replication protein a protein-protein interactions using a fragment-linking approach. J. Med. Chem. 56, 9242–9250.

Ge, X.Q., Jackson, D.A., Blow, J.J., 2007. Dormant origins licensed by excess Mcm2-7 are required for human cells to survive replicative stress. Genes Dev. 21, 3331–3341.

Glanzer, J.G., Liu, S., Oakley, G.G., 2011. Small molecule inhibitor of the RPA70 N-terminal protein interaction domain discovered using in silico and in vitro methods. Bioorg. Med. Chem. 19, 2589–2595.

Gotter, A.L., Suppa, C., Emanuel, B.S., 2007. Mammalian TIMELESS and Tipin are evolutionarily conserved replication fork-associated factors. J. Mol. Biol. 366, 36–52.

Green, C.M., Almouzni, G., 2003. Local action of the chromatin assembly factor CAF-1 at sites of nucleotide excision repair in vivo. EMBO J. 22, 5163–5174.

Holstege, H., Joosse, S.A., van Oostrom, C.T., Nederlof, P.M., de Vries, A., Jonkers, J., 2009. High incidence of protein-truncating TP53 mutations in BRCA1-related breast cancer. Cancer Res. 69, 3625–3633.

Kemp, M.G., Akan, Z., Yilmaz, S., Grillo, M., Smith-Roe, S.L., Kang, T.H., Cordeiro-Stone, M., Kaufmann, W.K., Abraham, R.T., Sancar, A., Unsal-Kacmaz, K., 2010. Tipin-replication protein A interaction mediates Chk1 phosphorylation by ATR in response to genotoxic stress. J. Biol. Chem. 285, 16562–16571.

Kenny, P.A., Lee, G.Y., Myers, C.A., Neve, R.M., Semeiks, J.R., Spellman, P.T., Lorenz, K., Lee, E.H., Barcellos-Hoff, M.H., Petersen, O.W., Gray, J.W., Bissell, M.J., 2007. The morphologies of breast cancer cell lines in three-dimensional assays correlate with their profiles of gene expression. Mol. Oncol. 1, 84–96.

Lecona, E., Fernandez-Capetillo, O., 2014. Replication stress and cancer: it takes two to tango. Exp. Cell Res. 329, 26–34.

Lee, G.Y., Kenny, P.A., Lee, E.H., Bissell, M.J., 2007. Three-dimensional culture models of normal and malignant breast epithelial cells. Nat. Methods 4, 359–365.

Lehmann, B.D., Bauer, J.A., Chen, X., Sanders, M.E., Chakravarthy, A.B., Shyr, Y., Pietenpol, J.A., 2011. Identification of human triple-negative breast cancer subtypes and preclinical models for selection of targeted therapies. J. Clin. Invest 121, 2750–2767.

Leman, A.R., Noguchi, C., Lee, C.Y., Noguchi, E., 2010. Human timeless and tipin stabilize replication forks and facilitate sister-chromatid cohesion. J. Cell Sci. 123, 660–670.

Liedtke, C., Mazouni, C., Hess, K.R., Andre, F., Tordai, A., Mejia, J.A., Symmans, W.F., Gonzalez-Angulo, A.M., Hennessy, B., Green, M., Cristofanilli, M., Hortobagyi, G.N., Pusztai, L., 2008. Response to neoadjuvant therapy and long-term survival in patients with triple-negative breast cancer. J. Clin. Oncol. 26, 1275–1281.

Lou, S., Luo, Y., Cheng, F., Huang, Q., Shen, W., Kleiboeker, S., Tisdale, J.F., Liu, Z., Qiu, J., 2012. Human parvovirus B19 DNA replication induces a DNA damage response that is dispensable for cell cycle arrest at phase G2/M. J. Virol. 86, 10748–10758.

Lukas, C., Falck, J., Bartkova, J., Bartek, J., Lukas, J., 2003. Distinct spatiotemporal dynamics of mammalian checkpoint regulators induced by DNA damage. Nat. Cell Biol. 5, 255–260.

Ma, C.X., Cai, S., Li, S., Ryan, C.E., Guo, Z., Schaiff, W.T., Lin, L., Hoog, J., Goiffon, R.J., Prat, A., Aft, R.L., Ellis, M.J., Piwnica-Worms, H., 2012. Targeting Chk1 in p53-deficient triple-negative breast cancer is therapeutically beneficial in human-in-mouse tumor models. J. Clin. Invest 122, 1541–1552.

Macheret, M., Halazonetis, T.D., 2015. DNA replication stress as a hallmark of cancer. Annu. Rev. Pathol. 10, 425–448.

Maire, V., Baldeyron, C., Richardson, M., Tesson, B., Vincent-Salomon, A., Gravier, E., Marty-Prouvost, B., De Koning, L., Rigaill, G., Dumont, A., Gentien, D., Barillot, E., Roman-Roman, S., Depil, S., Cruzalegui, F., Pierre, A., Tucker, G.C., Dubois, T., 2013a. TTK/hMPS1 is an attractive therapeutic target for triple-negative breast cancer. PLoS One 8, e63712.

Maire, V., Nemati, F., Richardson, M., Vincent-Salomon, A., Tesson, B., Rigaill, G., Gravier, E., Marty-Prouvost, B., De Koning, L., Lang, G., Gentien, D., Dumont, A., Barillot, E., Marangoni, E., Decaudin, D., Roman-Roman, S., Pierre, A., Cruzalegui, F., Depil, S., Tucker, G.C., Dubois, T., 2013b. Polo-like kinase 1: a potential therapeutic option in combination with conventional chemotherapy for the management of patients with triple-negative breast cancer. Cancer Res. 73, 813–823.

Manie, E., Vincent-Salomon, A., Lehmann-Che, J., Pierron, G., Turpin, E., Warcoin, M., Gruel, N., Lebigot, I., Sastre-Garau, X., Lidereau, R., Remenieras, A., Feunteun, J., Delattre, O., de The, H., Stoppa-Lyonnet, D., Stern, M.H., 2009. High frequency of TP53 mutation in BRCA1 and sporadic basal-like carcinomas but not in BRCA1 luminal breast tumors. Cancer Res. 69, 663–671.

Marty, B., Maire, V., Gravier, E., Rigaill, G., Vincent-Salomon, A., Kappler, M., Lebigot, I., Djelti, F., Tourdes, A., Gestraud, P., Hupe, P., Barillot, E., Cruzalegui, F., Tucker, G.C., Stern, M.H., Thiery, J.P., Hickman, J.A., Dubois, T., 2008. Frequent PTEN genomic alterations and activated phosphatidylinositol 3-kinase pathway in basal-like breast cancer cells. Breast Cancer Res. 10, R101.

Mazzoccoli, G., Piepoli, A., Carella, M., Panza, A., Pazienza, V., Benegiamo, G., Palumbo, O., Ranieri, E., 2012. Altered expression of the clock gene machinery in kidney cancer patients. Biomed. Pharmacother. 66, 175–179.

Merry, C., Fu, K., Wang, J., Yeh, I.J., Zhang, Y., 2010. Targeting the checkpoint kinase Chk1 in cancer therapy. Cell Cycle 9, 279–283.

Metzger-Filho, O., Tutt, A., de Azambuja, E., Saini, K.S., Viale, G., Loi, S., Bradbury, I., Bliss, J.M., Azim Jr., H.A., Ellis, P., Di Leo, A., Baselga, J., Sotiriou, C., Piccart-Gebhart, M., 2012. Dissecting the heterogeneity of triple-negative breast cancer. J. Clin. Oncol. 30, 1879–1887.

Meyer, B., Voss, K.O., Tobias, F., Jakob, B., Durante, M., Taucher-Scholz, G., 2013. Clustered DNA damage induces pan-nuclear H2AX phosphorylation mediated by ATM and DNA-PK. Nucleic Acids Res. 41, 6109–6118.

Ni, J., Liu, Q., Xie, S., Carlson, C., Von, T., Vogel, K., Riddle, S., Benes, C., Eck, M., Roberts, T., Gray, N., Zhao, J., 2012. Functional characterization of an isoform-selective inhibitor of PI3K-p110beta as a potential anticancer agent. Cancer Discov. 2, 425–433.

Popova, T., Manie, E., Rieunier, G., Caux-Moncoutier, V., Tirapo, C., Dubois, T., Delattre, O., Sigal-Zafrani, B., Bollet, M., Longy, M., Houdayer, C., Sastre-Garau, X., Vincent-Salomon, A., Stoppa-Lyonnet, D., Stern, M.H., 2012. Ploidy and large-scale genomic instability consistently identify basal-like breast carcinomas with BRCA1/2 inactivation. Cancer Res. 72, 5454–5462.

Quivy, J.P., Roche, D., Kirschner, D., Tagami, H., Nakatani, Y., Almouzni, G., 2004. A CAF-1 dependent pool of HP1 during heterochromatin duplication. EMBO J. 23, 3516–3526.

Raderschall, E., Golub, E.I., Haaf, T., 1999. Nuclear foci of mammalian recombination proteins are located at single-stranded DNA regions formed after DNA damage. Proc. Natl. Acad. Sci. U S A 96, 1921–1926.

Reaper, P.M., Griffiths, M.R., Long, J.M., Charrier, J.D., Maccormick, S., Charlton, P.A., Golec, J.M., Pollard, J.R., 2011. Selective killing of ATM- or p53-deficient cancer cells through inhibition of ATR. Nat. Chem. Biol. 7, 428–430.

Relles, D., Sendecki, J., Chipitsyna, G., Hyslop, T., Yeo, C.J., Arafat, H.A., 2013. Circadian gene expression and clinicopathologic correlates in pancreatic cancer. J. Gastrointest. Surg. 17, 443–450.

Rogakou, E.P., Boon, C., Redon, C., Bonner, W.M., 1999. Megabase chromatin domains involved in DNA double-strand breaks in vivo. J. Cell Biol. 146, 905–916.

Saal, L.H., Gruvberger-Saal, S.K., Persson, C., Lovgren, K., Jumppanen, M., Staaf, J., Jonsson, G., Pires, M.M., Maurer, M., Holm, K., Koujak, S., Subramaniyam, S., Vallon-Christersson, J., Olsson, H., Su, T., Memeo, L., Ludwig, T., Ethier, S.P., Krogh, M., Szabolcs, M., Murty, V.V., Isola, J., Hibshoosh, H., Parsons, R., Borg, A., 2008. Recurrent gross mutations of the PTEN tumor suppressor gene in breast cancers with deficient DSB repair. Nat. Genet. 40, 102–107.

Schepeler, T., Lamy, P., Hvidberg, V., Laurberg, J.R., Fristrup, N., Reinert, T., Bartkova, J., Tropia, L., Bartek, J., Halazonetis, T.D., Pan, C.C., Borre, M., Dyrskjot, L., Orntoft, T.F., 2013. A high resolution genomic portrait of bladder cancer: correlation between genomic aberrations and the DNA damage response. Oncogene 32, 3577–3586.

Schlacher, K., Christ, N., Siaud, N., Egashira, A., Wu, H., Jasin, M., 2011. Double-strand break repair-independent role for BRCA2 in blocking stalled replication fork degradation by MRE11. Cell 145, 529–542.

Schlacher, K., Wu, H., Jasin, M., 2012. A distinct replication fork protection pathway connects Fanconi anemia tumor suppressors to RAD51-BRCA1/2. Cancer Cell 22, 106–116.

Shah, S.P., Roth, A., Goya, R., Oloumi, A., Ha, G., Zhao, Y., Turashvili, G., Ding, J., Tse, K., Haffari, G., Bashashati, A., Prentice, L.M., Khattra, J., Burleigh, A., Yap, D., Bernard, V., McPherson, A., Shumansky, K., Crisan, A., Giuliany, R., Heravi-Moussavi, A., Rosner, J., Lai, D., Birol, I., Varhol, R., Tam, A., Dhalla, N., Zeng, T., Ma, K., Chan, S.K., Griffith, M., Moradian, A., Cheng, S.W., Morin, G.B., Watson, P., Gelmon, K., Chia, S., Chin, S.F., Curtis, C., Rueda, O.M., Pharoah, P.D., Damaraju, S., Mackey, J., Hoon, K., Harkins, T., Tadigotla, V., Sigaroudinia, M., Gascard, P., Tlsty, T., Costello, J.F., Meyer, I.M., Eaves, C.J., Wasserman, W.W., Jones, S., Huntsman, D., Hirst, M., Caldas, C., Marra, M.A., Aparicio, S., 2012. The clonal and mutational evolution spectrum of primary triple-negative breast cancers. Nature 486, 395–399.

Smith-Roe, S.L., Patel, S.S., Simpson, D.A., Zhou, Y.C., Rao, S., Ibrahim, J.G., Kaiser-Rogers, K.A., Cordeiro-Stone, M., Kaufmann, W.K., 2011. Timeless functions independently of the Tim-Tipin complex to promote sister chromatid cohesion in normal human fibroblasts. Cell Cycle 10, 1618–1624.

Smith-Roe, S.L., Patel, S.S., Zhou, Y., Simpson, D.A., Rao, S., Ibrahim, J.G., Cordeiro-Stone, M., Kaufmann, W.K., 2013. Separation of intra-S checkpoint protein contributions to DNA replication fork protection and genomic stability in normal human fibroblasts. Cell Cycle 12, 332–345.

Smith, K.D., Fu, M.A., Brown, E.J., 2009. Tim-Tipin dysfunction creates an indispensible reliance on the ATR-Chk1 pathway for continued DNA synthesis. J. Cell Biol. 187, 15–23.

Sorlie, T., Perou, C.M., Tibshirani, R., Aas, T., Geisler, S., Johnsen, H., Hastie, T., Eisen, M.B., van de Rijn, M., Jeffrey, S.S., Thorsen, T., Quist, H., Matese, J.C., Brown, P.O., Botstein, D., Eystein Lonning, P., Borresen-Dale, A.L., 2001. Gene expression patterns of breast carcinomas distinguish tumor subclasses with clinical implications. Proc. Natl. Acad. Sci. U S A 98, 10869–10874.

Stemke-Hale, K., Gonzalez-Angulo, A.M., Lluch, A., Neve, R.M., Kuo, W.L., Davies, M., Carey, M., Hu, Z., Guan, Y., Sahin, A., Symmans, W.F., Pusztai, L., Nolden, L.K., Horlings, H., Berns, K., Hung, M.C., van de Vijver, M.J., Valero, V., Gray, J.W., Bernards, R., Mills, G.B., Hennessy, B.T., 2008. An integrative genomic and proteomic analysis of PIK3CA, PTEN, and AKT mutations in breast cancer. Cancer Res. 68, 6084–6091.

Techer, H., Koundrioukoff, S., Azar, D., Wilhelm, T., Carignon, S., Brison, O., Debatisse, M., Le Tallec, B., 2013. Replication dynamics: biases and robustness of DNA fiber analysis. J. Mol. Biol. 425, 4845–4855.

Toledo, L.I., Murga, M., Gutierrez-Martinez, P., Soria, R., Fernandez-Capetillo, O., 2008. ATR signaling can drive cells into senescence in the absence of DNA breaks. Genes Dev. 22, 297–302.

Toledo, L.I., Murga, M., Zur, R., Soria, R., Rodriguez, A., Martinez, S., Oyarzabal, J., Pastor, J., Bischoff, J.R., Fernandez-Capetillo, O., 2011. A cell-based screen identifies ATR inhibitors with synthetic lethal properties for cancer-associated mutations. Nat. Struct. Mol. Biol. 18, 721–727.

Tourriere, H., Pasero, P., 2007. Maintenance of fork integrity at damaged DNA and natural pause sites. DNA Repair (Amst) 6, 900–913.

Turner, N., Tutt, A., Ashworth, A., 2004. Hallmarks of 'BRCAness' in sporadic cancers. Nat. Rev. Cancer 4, 814–819.

Turner, N.C., Reis-Filho, J.S., 2013. Tackling the diversity of triple-negative breast cancer. Clin. Cancer Res. 19, 6380–6388.

Unsal-Kacmaz, K., Chastain, P.D., Qu, P.P., Minoo, P., Cordeiro-Stone, M., Sancar, A., Kaufmann, W.K., 2007. The human Tim/Tipin complex coordinates an intra-S checkpoint response to UV that slows replication fork displacement. Mol. Cell Biol. 27, 3131–3142.

Urtishak, K.A., Smith, K.D., Chanoux, R.A., Greenberg, R.A., Johnson, F.B., Brown, E.J., 2009. Timeless maintains genomic stability and suppresses sister chromatid exchange during unperturbed DNA replication. J. Biol. Chem. 284, 8777–8785.

Workman, P., Aboagye, E.O., Balkwill, F., Balmain, A., Bruder, G., Chaplin, D.J., Double, J.A., Everitt, J., Farningham, D.A., Glennie, M.J., Kelland, L.R., Robinson, V., Stratford, I.J., Tozer, G.M., Watson, S., Wedge, S.R., Eccles, S.A., Committee

of the National Cancer Research, I, 2010. Guidelines for the welfare and use of animals in cancer research. Br. J. Cancer 102, 1555–1577.

Yoshida, K., Sato, M., Hase, T., Elshazley, M., Yamashita, R., Usami, N., Taniguchi, T., Yokoi, K., Nakamura, S., Kondo, M., Girard, L., Minna, J.D., Hasegawa, Y., 2013. TIMELESS is overexpressed in lung cancer and its expression correlates with poor patient survival. Cancer Sci. 104, 171–177.

Yoshizawa-Sugata, N., Masai, H., 2007. Human Tim/Timeless-interacting protein, Tipin, is required for efficient progression of S phase and DNA replication checkpoint. J. Biol. Chem. 282, 2729–2740.